Design Considerations for Digital Light Processing Bioprinters

Carlos Ezio Garciamendez-Mijares ¹⁺, Francisco Javier Aguilar ¹⁺, Pavel Hernandez ^{1#}, Xiao Kuang ^{1#}, Mauricio Gonzalez ^{1#}, Vanessa Ortiz ^{1#}, Ricardo A. Riesgo ^{1#}, David S. Rendon Ruiz ¹, Victoria Abril Manjarrez Rivera ¹, Juan Carlos Rodriguez ¹, Francisco Lugo Mestre ¹, Penelope Ceron Castillo ¹, Abraham Perez ¹, Lourdes Monserrat Cruz ¹, Khoon S. Lim ², Yu Shrike Zhang ^{1*}

- + Equally contributing first authors
- # Equally contributing second authors

¹ Division of Engineering in Medicine, Department of Medicine, Brigham and Women's Hospital, Harvard Medical School, Cambridge, MA 02139, USA

² School of Medical Sciences, University of Sydney, Sydney 2006, Australia

^{*} Corresponding author: <u>yszhang@bwh.harvard.edu</u>

ABSTRACT

With the rapid development and popularization of additive manufacturing (AM), different technologies, including but not limited to extrusion-, droplet-, and vat-photopolymerization-based fabrication techniques, have emerged that have allowed tremendous progress in 3D printing in the past decades. Bioprinting, typically using living cells and/or biomaterials conformed by different printing modalities, has produced functional tissues. As a subclass of vat-photopolymerization printing, digital light processing (DLP) uses digitally controlled photomasks to selectively solidify liquid photocurable bioinks to construct complex physical objects in a layer-by-layer manner. DLP printing presents unique advantages, including short printing times, relatively low manufacturing costs, and decently high resolutions, allowing users to achieve significant progress in the bioprinting of tissue-like complex structures. Nevertheless, the need to accommodate different materials while bioprinting and improve the printing performance has driven the rapid progress in DLP bioprinters, which requires multiple pieces of knowledge ranging from optics, electronics, software, and materials beyond the biological aspects. This raises the need for a comprehensive review to recapitulate the most important considerations in the design and assembly of DLP bioprinters. This review begins with analyzing unique considerations and specific examples in the hardware, including the resin vat, optical system, and electronics. In the software, the workflow is analyzed, including the parameters to be considered for the control of the bioprinter and the voxelizing/slicing algorithm. In addition, we briefly discuss the material requirements for DLP bioprinting. Then, we provide a section with best practices and maintenance of a do-it-yourself (DiY) DLP bioprinter. Finally, we highlight the future outlooks of the DLP technology and their critical role in directing the future of bioprinting. The state-of-the-art progress in DLP bioprinter in this review will provide a set of knowledge for innovative DLP bioprinter designs.

Keywords: Digital light processing (DLP); vat-photopolymerization; additive manufacturing (AM); bioprinting; bioprinter; design; do-it-yourself (DiY)

1 INTRODUCTION

Additive manufacturing (AM), or 3D printing, has become a disruptive technology for advanced manufacturing, consequently expanding applications since its first development in the 1980s ^{1,2}. AM is a technology that enables the creation of 2D or 3D objects in an additive way instead of a subtractive manner. In a typical 3D printing process, a target object is transformed into digital data utilizing 3D scanning or/and a computer-aided design (CAD) model, which is sliced into layered data or toolpaths to guide the automated ink/material deposition using the AM machine (or 3D printer) often in a layer-by-layer manner. AM holds several advantages, including geometrical complexity with high precision, reducing material waste, flexibility in design, personalization, and customization over traditional techniques ³. For these reasons, AM has rapidly grown, and its influence is seen in many fields, including rapid prototyping, electronics, aerospace, medical devices, and tissue engineering ².

The intrinsic attribute of personalization makes 3D printing suitable for biomedical applications. Notably, 3D bioprinting offers a reproducible, scalable, and precise fabrication of 3D anatomical living tissues or models for broad biotechnologies ⁴⁻⁶. Bioprinting is a process that uses bioinks, consisting of living cells and/or biodegradable biomaterials, sometimes also other bioactive components, to print engineered biofunctional constructs ⁷. In the past decades, various bioinks and bioprinting modalities have been developed to create tissue implants (e.g., bone, skin, cartilage) ⁵, aid the fabrication of organ-on-chip devices ⁸, and generate physiologically relevant structures for drug development and disease modeling 9-11. Based on bioink disposition and solidification methods, bioprinting techniques can be classified into extrusion-, droplet-, and vatphotopolymerization-based bioprinting. There are several different derivatives and subclasses of modalities for each technique. For example, vat-photopolymerization-based modalities include stereolithography apparatus (SLA), digital light processing (DLP), and volumetric AM ^{6,12}. DLP bioprinting is particularly interesting as it shows certain advantages, including generally fast printing speeds, decently high print resolutions, and relatively low fabrication costs ¹³. Due to these reasons, users have been working on new designs and developments to further expand the possibilities of this technique for laboratories and commercial companies ¹⁴.

In DLP bioprinting, digital photomasks are successfully displayed to selectively solidify a liquid photocurable bioink and build the construct in a layer-by-layer manner. DLP uses a light modulator of digital micromirror devices (DMDs) that digitally control high-resolution pixelated

light patterns. In a typical bottom-up DLP bioprinting, the light source is positioned below the bioink vat, and the light is directed upward onto a transparent window made of a low-adhesion material, such as fluorinated ethylene propylene (FEP) films. During printing, the first layer of the part is cured and adheres firmly to the build-platform surface. The build stage moves up and separates from the vat window, and the subsequent layers are cured onto the previous layers until the whole model is printed. Typically, the minimum resolution of DLP-based 3D printing can range from few to 50 µm ¹². With some significant advances made to the AM field in the early 2000s ¹⁵, and in 2015, one of the prior research works of DLP bioprinting showcased the ability to create physiologically relevant liver-like structures ¹⁶. Since then, there has been more progress in bioprinting applications; for example, fabricating liver microtissues ¹⁷, creating hydrogel models of lung-simulating air sacs ¹⁸, and producing bone tissue scaffolds ¹⁹. Recently, new DLPderivative techniques, such as fast hydrogel stereolithography printing (FLOAT), have emerged and significantly improved the printing performance with faster speed and larger size 20. All this progress, derived from the interdisciplinary development of DLP printers and bioinks, can better meet the needs of various biomedical applications. Therefore, the need to develop a review that outlines the primary considerations when designing a DLP bioprinter arises from all these advances. The design of this kind of system requires different areas of specialization, ranging from mechanical, optical, electronics, and software to materials and cells. This work provides readers with a comprehensive review of the development of DLP bioprinters for various purposes.

Herein, we provide new or experienced users with the necessary tools to develop any generic, specific, or novel DLP bioprinter design to best fit their application needs. In this review, we mainly elaborate on the five components in the DLP bioprinter design (illustrated and summarized in **Fig. 1**): hardware (further divided into stage and resin vat, optics, electronics), software, and materials. First, some considerations for the stage and vat are presented, as well as some specific examples and how they could impact the functionality of a DLP bioprinter. Next, we delve deeper into basic optical principles and provides information on commonly used light sources, DMDs, and optical components. Following this, the electronics that comprise the design of a bioprinter are explored, specifically motors and motor-drivers, position-sensors, controllers, and power sources. Additionally, the software workflow (selection of parameters, generation of images, and synchronization) is presented, wherein voxelization, slicing processes, and open-source alternatives are further discussed. Moreover, we briefly cover fundamental material design

principles and provide recent examples of bioinks utilized for DLP bioprinting. Lastly, a depiction of best practices and maintenance procedures for a do-it-yourself (DiY) DLP bioprinter is given; and we also highlight prospective trends for next-generation high-performance vat-photopolymerization bioprinting.

2 STAGE AND RESIN VAT

When designing a DLP bioprinter, the first step is selecting the configuration to use, which could be bottom-up or top-down. The main difference between these two configurations is the direction of the light emittance with respect to the stage and vat and the displacement direction of the stage. The bottom-up configuration emanates the light from beneath the vat, passing through an optically transparent film located at the bottom of the resin vat, with the stage moving in the upward direction; the printed construct adheres to the stage upside-down ²¹. In the top-down configuration, light emanates from the top with respect to the stage and vat, and the stage moves downward; the printed construct adheres to the stage upright ²². It is important to note that the configuration choice is primarily influenced by the bioink's properties, such as viscosity, quantity, and integrity, or by specific application needs, i.e., the structure to be bioprinted. Bioinks with high viscosities often pose challenges in the bottom-up approach, as the drag forces exerted can cause the structures to detach or distort ²³. The quantity of the bioink also plays a critical role; even with minimal material quantities, such as a single drop ²⁴, the bottom-up approach remains feasible, whereas top-down approaches are unsuitable in such scenarios ^{23,24}. Furthermore, the integrity of the material is crucial. Printing an ultra-soft, porous material poses significant challenges with the bottom-up configuration due to the pulling forces that often result in failed prints; thus, only the top-down configuration is viable ²⁵. Lastly, the aspect ratio of the desired structure influences the choice of configuration. If the structure is significantly taller than it is wide, the bottom-up approach may lead to fissures; conversely, if the structure is wider than it is tall, the top-down approach may result in less homogeneous bioprinted layers ²³. For further discussions behind the criteria for selecting the appropriate configuration (that is depending on bioink properties) the reader is referred to key related works ^{12,22,23,26,27}.

After determining the configuration to be used, the next step is to understand the relationship between the stage and the resin vat since they work together, or in synchrony, complementing and influencing each other during bioprinting ^{22,26,28,29}. As an example of their synchronicity, in the

bottom-up configuration, it is desired to have proper print adhesion to the stage, which is also influenced by the separation forces at the resin vat; therefore, favorable stage adhesion is aided by positive vat separation (**Fig. 2A**) ^{22,28,29}. On the other hand, for top-down, the movement of the stage as it submerges itself and the construct into the vat full of bioink during the photocrosslinking of successive layers can create a lack of uniformity on the surface, which affects the layer thickness consistency throughout the bioprinting process (**Fig. 2B**) ³⁰.

Once the first two steps (bioprinter configuration selection and understanding the synergy between components) the stage and resin vat design are complete, there are some other key points to consider for proper stage and vat designs. For the bottom-up configuration, these points include: sufficient stage adhesion (**Fig. 2A i**), influenced by surface physicochemical properties (**Fig. 2A ii**), and proper layer-separation by reducing the vacuum/suction forces (**Fig. 2A iii**), influenced by the creation of a dead zone (zone of uncurable bioink above the film's surface) *via* the film's oxygen-permeability (**Fig. 2A iv**). The key point in the top-down configuration is consistent layer thickness (**Fig. 2B i**), for which the recoating system (**Fig. 2B ii**) takes an important part and will be further explored as well ^{26,31,32}.

In the following sections, some generic and unique considerations for the design of the stage and the resin vat are further analyzed, each followed by an overview of specific examples, determined by novelty or applicability to bioprinting. The research projects from where these examples originated have been (mostly) applied in a 3D printing context. Therefore, we aim not only to analyze the functionality of the designs but also to provide examples for translating these designs from the 3D printing sphere to the bioprinting realm. Furthermore, a summary of pivotal multi-material demonstrations is also presented. For reference, we refer to the 3D printers used to develop these designs as bioprinters and printing as bioprinting for ease of presentation; it is also clarified whether cells have been used (or not) where applicable.

2.1 Stage

The stage, also known as the build platform, is fundamental in the DLP bioprinting workflow as it is the surface to which the printed construct will adhere. Some generic characteristics relevant to the stage's design are cytocompatibility, leveling, and surface. The first and most fundamental aspect in creating the stage, specifically for DLP bioprinting, is the cytocompatibility of the stage's surface, as it must be non-toxic for cells and prevent any contamination ³². Sterilizing the surface

may provide a non-contaminating environment for the bioinks to adhere to. Some conventional solid surface sterilization methods include ultraviolet (UV) illumination before bioprinting (at least 30 minutes) and ethanol solution washing ^{33,34}. The second consideration for the stage design is the correct leveling of the surface onto which the print will adhere; this is important because it helps to avoid deformation on the print or even failure during the printing process. For proper stage leveling, it is recommended to have a clean surface, calibrate the mechanical and electronic components, and perform machine maintenance as needed. To that end, if the bioprinter has been modified from a commercial printer, the manufacturer might provide a manual for proper calibration and maintenance. Additionally, position-sensors can help ensure that the stage is in the correct position when initializing printing. Notably, surface of the stage is also important, as it has varying degrees of relevance depending on the configuration employed.

2.1.1 Generic stage considerations

A rough stage surface finish is most prevalent in bottom-up configurations since it increases the contact area and allows mechanical interlocking between the stage and the print, providing proper adhesion (**Fig. 2A ii**). This, in turn, prevents print detachment, which may cause defects or even complete decoupling between the print and the stage (**Fig. 2A i**) ²². The surface roughness acts as small pockets that make up the stage's surface and clasp onto the crosslinked (base-layer) bioink, ensuring print adhesion to the stage throughout the bioprinting workflow ²⁸. During the motion of the stage, a pressure difference/vacuum is generated between the newly crosslinked layer (bioink) and the film/bottom of the vat, creating a tiny gap. The uncured bioink is unable to fill the said gap, generating a suction force that can cause printing defects, such as detachment, holes in final prints, excessive layer adhesion to the stage, and broken prints, to name a few ^{26,28,29}. This problem can be tackled by proper stage-print adhesion, *e.g.*, having a rough stage surface, and by considering resin vat design choices that promote suitable layer separation ^{26,29}.

Moreover, building the overall design of the stage with the foresight to couple a tool or mechanism for the detachment of the print can be of aid. For example, an elegant commercially available solution for print detachment is a flexible demolding mechanism for the stage. Some companies have developed custom third-party accessories for certain commercial printers, such as 3D-printed tilted stage-holders for recovering excess uncured material after finishing a print. Though the previously mentioned solutions are not bioprinting oriented, a trend can be seen of

increased commercial DLP bioprinting solutions being introduced to the market. Therefore, commercial solutions with additional features, such as the demolding mechanism, may exist soon and could be bought and incorporated into the bioprinter design.

Of note, in the top-down configuration, when the stage moves downwards, and the final print adheres upright, adhesion does not work against the vacuum forces acting on the structure as the part gets pulled up in the bottom-up configuration; therefore, print detachment issues are not as common, yet should still be accounted for ^{23,29}.

2.1.2 Specific stage examples

The first examples to be analyzed constitute a simple design that can be easily reproduced. Some research works illustrate the ability to use glass, a commonly used material, as the stage's surface and showed satisfactory print adhesion (**Fig. 3A**) ^{27,35}. In these projects, the bottom of the stage was coupled with a glass building plate where the print would adhere. One primary motivation behind using glass was to enhance the interface bonding with the hydrogel materials produced. Another interesting note related to these research works is the generic, effective, and reproducible stage designs utilized; such stage designs can be easily replicated or found on platforms with online 3D computer-aided design (CAD) libraries, such as GrabCAD.

Proper layer separation also influences print adhesion to the stage; a novel stage design termed injection continuous liquid interface production (iCLIP) aims to enhance layer separation *via* the stage ³⁶. This technique was able to design a microfluidic stage wherein a channel injects pressurized bioink from internally while printing (**Fig. 3B**). With iCLIP, it is possible to deliver bioink at specific points to counteract some of the suction forces, and it is also useful for multimaterial bioprinting, allowing for the creation of increasingly complex constructs. Multi-material DLP is an area of significant interest in bioprinting due to the possibility of creating complex bioactive structures ³⁷. For further information about multi-material purposes and applications, the reader can refer to reviews on this topic ^{12,38}. Although biological applications were not delved into in iCLIP, *i.e.*, no cells were used the multi-material functionality presented could easily be extrapolated into the bioprinting field by using different types of bioinks in a construct as well as enabling fast(er) DLP bioprinting.

Moreover, the ability to bioprint increasingly complex constructs is a constant necessity to emulate the natural structures and organization of tissues, organs, and drug-testing platforms ^{33,39}–

⁴². In one example, complex prints with conformal geometries were achieved by incorporating a 6-degree-of-freedom (DOF) robotic arm as the DLP bioprinter's stage (**Fig. 3C**) ⁴³. Although this example did not expand upon work related to cells, the relationship with bioprinting is easily identifiable. This report highlights the ability to print complex structures without needing support; the added freedom would be pivotal for bioprinting constructs since complex hollow channels (a key benefit of DLP bioprinting) could be produced without internal support. The relevance of this work is further heightened by its multi-vat functionalities that allow for multi-material bioprinting.

Displayed in **Fig. 3D** is another exemplification with a distinctive modification, by utilizing a delta 3D printer onto which the stage was mounted, coupled with an additional rotational axis ⁴⁴. This demonstration did not explore cell-related work, yet its translation for bioprinting applications could prove helpful. Employing such a mechanism provides freedom for creating larger-scale prints by implementing stitching, which combines multiple projection images into one to account for a larger projection area. This technique enables DLP bioprinting with a larger print area without losing the resolution. Another noteworthy characteristic of this work was implementing a tilting mechanism for better print detachment between the stage and the vat.

Another recent example had a unique approach to fabricate multi-material structures, combining multiple techniques – specifically, integrating top-down DLP with extrusion (**Fig. 3E**) ⁴⁵. Of note, this work did not delve into biological applications or bioinks. Nevertheless, this approach would enable users to have a broader range of bioink selection; extrusion bioprinting would permit the fabrication of constructs from viscous bioinks ^{12,46}, while top-down DLP bioprinting would allow the generation of softer constructs from low-viscosity bioinks ²³. This combination of DLP with extrusion not only harnesses the unique advantages of each but also compensates for their respective limitations, making it a promising development for bioprinting and tissue engineering.

2.2 Resin Vat

In a DLP bioprinter, the resin vat, or resin reservoir, is a container for the bioink and is pivotal in the bioprinting workflow. Vat designs must consider multiple elements, some generic and others specific to the configuration (bottom-up or top-down) used. The critical difference is that in the bottom-up configuration, the vat will also include a transparent film at the bottom.

Similar to the stage, general important characteristics include sterility and leveling. Sterility is essential for preventing bioink contamination in 3D DLP bioprinting ³², and sterilization of the resin vat is crucial to create and maintain an aseptic environment for cells. The previously mentioned sterilization strategies can also be employed for the vat; however, sterilization techniques such as ethanol and heat should be applied only as permitted per film material to avoid damage to the film. Additionally, the leveling of the resin vat is mainly affected by the bioprinter's general leveling. Typically, no significant modifications or additions are needed for a leveled vat other than proper installation and assembly. To achieve this, some commercial products use feet leveling and an interactive leveling sensor to ensure correct alignment.

2.2.1 Generic resin vat considerations

Analyzing the bottom-up configuration, the main consideration for the resin vat design is selecting the correct film at the bottom, which depends on optical transparency and reduction of vacuum/suction forces. An optically transparent film is necessary since it allows the light emitted from below the resin vat to pass through and interact with the bioink to enable the crosslinking of the layers ²⁸. Of note, the film's optical transparency should be in the same range as the chosen optical wavelength. Another important consideration for the film should be the reduction of the vacuum/suction forces (Fig. 2A iii) that form between the uncured bioink and the crosslinked structure each time the stage begins to move in the upward direction, thus potentially affecting the final construct's quality, accuracy, and integrity ^{47,48}. One way to reduce these forces is by selecting a film with oxygen-permeability that accumulates a thin sheet of oxygen above the film's surface, inhibiting crosslinking in this area and creating a dead zone (Fig. 2A iv) ^{36,49}. Consequently, this will substantially reduce the adhesion to the film and facilitate easy separation. It is worth mentioning that other mechanisms can be implemented to minimize vacuum/suction forces, including peeling ⁵⁰, tilting ⁴⁴, and rotation ⁵¹ mechanisms, as well as utilizing dual-wavelength to inhibit crosslinking at the film's surface ⁴⁹. Additionally, innovative film materials and strategies, including fluorinated oil swollen gel ⁵², low-surface tension coatings ^{53–55}, and mobile oil interface ^{48,49}, among others, have been reported for use. However, their development has not been primarily demonstrated with cells, so some considerations must be made (i.e., ensuring that the flowing oil is benign to cells).

Several materials can be utilized as films, one being anti-stick films. These films are commonly used in DLP bioprinting, and some of the most important characteristics to look for when selecting a suitable anti-stick film are optically transparent, oxygen-permeable, chemically inert, wrinklefree, and swelling-resistance 51. These factors influence the DLP bioprinting workflow since a resin vat's film constantly interacts with the bioink, e.g., the presence of wrinkles and permanent deformations on the film can affect the print surface quality and dimensional accuracy. Teflon and fluorinated ethylene propylene (FEP) are anti-stick film materials used extensively ^{56–59}. In the first instance, Teflon AF2400 is a sensitive material that must be installed precisely to avoid any leakage and air bubbles trapped between the film and the resin vat. On the other hand, FEP films must also be installed carefully; however, this material is wrinkle-free and has better UV transmissivity than Teflon ⁵¹. Both films can be commonly found with distributors of commercial 3D DLP printers ⁵⁷. Other membranes are also an alternative to anti-stick films since they provide optical transparency; one material that has been used as a membrane is flexible silicone since its mechanical properties are easily tunable. In simplified terms, the thicker the membrane, the less flexible it becomes (i.e., the less it bends) and, therefore, the smaller the (pull) force required to break the suction/vacuum forces ⁴⁷. Polydimethylsiloxane (PDMS) membranes are also an excellent alternative to anti-stick films, particularly Teflon, since PDMS is more cost-effective, widely available, and commonly used ^{44,48,51,53}. One research work compared different anti-stick films and membranes, among them Teflon and PDMS, and analyzed the thickness of the generated dead zone during printing 60. Furthermore, additional research efforts have also highlighted the potential of using an additional PDMS coating with a horizontally moving stage to help with print separation from the film, a term coined the two-channel method ^{54,55}.

Regarding the top-down configuration, due to the light emitted from above, the design of the resin vat does not need a film or additional components. A key consideration for this configuration is the recoating system, which can be defined as the process of evenly distributing the uncured bioink on top of the newly crosslinked layer ⁶¹. In top-down bioprinting, when the stage and print are submerged in the bioink, this can cause difficulties in controlling and keeping precise and constant layer heights (**Fig. 2B i**) ^{12,22,31,61}. Several techniques for recoating have been developed to aid uniformity and consistency in the print's layer height, such as bounce and scrape ⁶². The bounce-and-scrape method has been used in top-down DLP bioprinters ^{62,63}; it consists of the print being submerged below the desired layer height (bounce), then adjusting upward below the surface

of the bioink to the selected layer height; lastly, a blade, or wiper, sweeps (i.e., scrapes) across the vat to remove excess and make the layer as uniform and smooth as possible (Fig. 2B ii) 64. It is worth mentioning that the velocity at which the wiper moves must be calibrated carefully. The intended goal is to achieve uniformity in the least amount of time possible without causing disruptions to the bioink (uniformity or cellular viability) ⁶⁵. Similarly, alternatives for the bounce and scrape have been developed for the redistribution of the bioink: deposit and scrape, scrape from tank, air knife, or even a vacuum reservoir at the center of the blade, i.e., Zephyr blade ^{61,63}. As previously stated, adaptations and considerations must be made to work with cells, i.e., ensuring the wiper is not exerting excessive pressure during the redistribution process. Therefore, a solution that is simple enough to reproduce is adding a bounce function by itself since it requires no additional components (wipers/blades). Several parameters must be accounted for during the implementation of the bounce, *i.e.*, height, speed, and light-off time, ⁶³. Nevertheless, incorporating just a bounce or adding the strategies mentioned above to a top-down vat can help homogeneously recoat the print. Some of these implementations can also be implemented in the bottom-up configuration, specifically bounce and bounce-and-scrape. For example, some commercial products utilize a bounce-and-scrape method in their resin vat to remove any excess material; this could be beneficial to ensure consistent layers during printing.

Certain companies provide low-cost resin vats that are available for purchase; these commercial solutions can be directly used or modified to work with a DLP bioprinter. Notably, these vats are designed to work with conventional resins (no cells used). Therefore, the total capacity (mL) needed to cure one layer evenly can be several (>15) mL, making them impractical to use with bioprinters. Nevertheless, by customizing the resin vat, it can be easily incorporated into a bioprinter. Bridging the gap between low-cost, commercially available materials and biological applications, a research project successfully repurposed a commercial vat to work with cells, a clear example of the adaptability and utility of commercial components ⁶⁶. A more cost-effective approach is implementing one of several open-source initiatives for vat designs; a popular one is FlexVat, which is commonly used in open-source bioprinters.

2.2.2 Specific resin vat examples

Regulation of bioink temperature is crucial to promote printability and viability. On one hand, cells prefer a temperature around 37 °C; simultaneously, certain bioink's viscosity can be more

favorably controlled at specific temperatures. To address this, a commercially available modification for the vat can be purchased, which is termed ThermalVatBand (**Fig. 4A**). This is an electric band that encircles a bioprinter's vat and helps heat the bioink *via* the vat's walls to the desired temperature values. An open-source project with a similar outcome utilized an indium-tin-oxide-heated platform at the bottom of the vat ⁶⁷. This approach could be implemented to reduce the viscosity of bioinks, which are not printable at ambient conditions, while ensuring benign temperature conditions for the cells.

Several methods exist to promote print separation, including the generation of a dead zone. One specific example, termed continuous liquid interface production (CLIP) 49, reduced vacuum/suction forces thanks to an oxygen-permeable film, enabling continuous printing, and increasing print speed by creating a dead zone via the oxygen-permeable film. Another way to assist print separation is by utilizing the oil flow. Another work expanded upon the concept of faster, continuous printing, termed high-area rapid printing (HARP), which consisted of providing a constant flow of fluorinated oil between the bottom of the vat and the ink to decrease the acting adhesion forces (Fig. 4B) ⁶⁸. Since HARP does not require an oxygenated dead zone, oxygensensitive and oxygen-insensitive materials could be used. To translate HARP into the bioprinting field, it is essential to consider that the oil used must also be biocompatible and not affect cell viability. Like the HARP technique, the fluid-supported liquid interface polymerization (FLIP) approach also utilized oil to promote print separation ⁶⁹. This was achieved by adding a reservoir to the bioprinter's vat, and then it injected a combination of crosslinkable bioink and support fluid (perfluorinated oil) during the bioprinting process. While utilizing FLIP, the support fluid gradually lifted the bioink and allowed crosslinking without needing a solid printing stage since it created a fluid layer that acted as one.

Other unique approaches have employed a microfluidics-based vat that enables multi-material printing. Different bioinks are pumped into a microfluidic resin vat in a project that we developed, achieving layer-by-layer multi-material printing ⁷⁰. This setup was later expanded upon, also by us, by incorporating a static mixer into the microfluidic vat, which enabled precise DLP bioprinting of complex gradient structures ⁵⁶. This was achieved by individually controlling the flow rates of different bioinks in the static mixer prior to reaching the vat; thus, regulating the mixed proportions of the bioinks while bioprinting (**Fig. 4C**). A more recent approach, developed by us, coupled bubble-generating microfluidics with the vat to fabricate porous structures ²⁵.

Another multi-material method seen in DLP bioprinting is multi-vat, which consists of having interchangeable vats to switch between multiple bioinks. Multi-vat can be arranged in a rotating ^{71,72} or linear configuration ^{35,43,73}. In the rotating configuration, a project showcased a design with interchangeable vats placed in a rotating carousel for a bioprinter with a top-down configuration (**Fig. 4D**) ⁷². This system crosslinked a layer with one bioink and afterward switched to a different vat to continue printing a subsequent layer with another bioink. Furthermore, another effort showed such a design integrated into multiple other systems for additional functions and was ultimately used in nerve-regeneration experiments ⁷⁴. In the linear configuration of the multi-vat system, vertical and horizontal arrangements have been delved into; a report has showcased interchangeable resin vats in a tower design to interchange the bioinks in a vertical manner; the system included two towers, one for storage and the other one for retrieval of the vats ⁷³. Other works demonstrated variations of the linear multi-vat systems, where the resin vats and a washing station are displaced in the horizontal direction ^{35,43}. Notably, the movement and alignment of these vats must be appropriately synchronized with the projection.

To overcome some of the challenges seen in DLP bioprinting, specifically the generation of support structures, a research work developed a dynamic support bath (**Fig. 4E**) ⁷⁵. The bath facilitated the placement and removal of supports. This occurred because the support bath was mixed in with the bioink while bioprinting, and the support bath could be easily removed during post-processing by applying a temperature of 37 °C for 60 minutes. This mechanism could provide users with the ability to create complex structures, often needing support, in a more straightforward way for cell applications.

3 OPTICS

When constructing the optics for a DLP bioprinter, the light-processing system is the mechanism that enables the precise projection of the desired images. DLP bioprinters are a subclass of the vat-polymerization technique, in which a specified distribution of energy, in the form of light, is projected onto a photocurable precursor, thus enabling the creation of 3D constructs in a layer-by-layer manner ^{6,40,76–79}. Typically, this is achieved with an optical setup composed of three subsystems: a light source, a DMD, and various optical components. In the following section, we will discuss these subsystems in further detail: their functions, main features,

specific examples, and important considerations when developing a DLP bioprinter. A complete overview of an optical setup that comprises a DLP bioprinter is illustrated in **Fig. 5**.

3.1 Light Source

The light source is where the light originates and whose energy intensity, output power, and wavelength are selected according to the desired values. Typical light sources utilized in DLP bioprinters are lasers, laser diodes, and light-emitting diodes (LEDs) ^{56,80,81} (**Fig. 5**). In addition, projectors are systems that already have an integrated light source and are also prevalent ^{81–85}. Some critical factors to consider when selecting these light sources (including the projector) are the working wavelength value, light intensity (i.e., output power), and spectral bandwidth (i.e., the wavelength range of a source at half of its light intensity). Wavelength is a physical property of light related to the individual energy of the photons composing the light beams. Wavelengths in the 10-380 nm range are said to be in the ultraviolet (UV) range, 380-760 nm form the visiblelight range, and 750 nm-1 mm are in the infrared range (IR) according to ISO 20473. Notably, in additive manufacturing that focuses on biomedical applications, the UV spectrum can be up to 405 nm ^{81,85}. **Table 1** compares the various light sources by analyzing three key aspects: luminous intensity (light intensity by unit area), spectral bandwidth, and approximated costs. Notably, when selecting a light source, it is crucial to consider how wavelength and light intensity impact cell viability ⁸⁶. For instance, one study demonstrated that prolonged UV exposure can be harmful to cell viability ⁸⁷. Moreover, some examples illustrate that increased luminous intensity can also compromise cell viability, seen with both UV and visible light wavelengths ^{88,89}. Therefore, careful consideration must be given to the wavelength and light intensity of the chosen light source to ensure optimal cell viability. The following section delves deeper into a detailed comparison of light sources, provides specific examples, and discusses how their characteristics could impact cell viability.

3.1.1 Comparison of different light sources

The resin polymerization rate is determined by the amount of energy it receives in addition to an absorption wavelength ⁹⁰. Hence, for faster DLP bioprinting, it is desirable to have a sufficiently high light intensity and a narrow spectral bandwidth centered around the specific working wavelength value (depending on the chosen photoinitiator/photoabsorber). Lasers are light sources

that radiate high energy, as well as rays with low spectral bandwidth, making them a great candidate as a bioprinter's light source 91-93. Furthermore, as a source of narrow spectral bandwidth, it employs a high spatial resolution, often utilized in nanometric resolution applications such as two-photon polymerization (TPP) bioprinting when two lasers are combined ^{94,95}. However, lasers with high light intensities of 10¹⁴-10¹⁵ W cm⁻² 96 and narrow spectral bandwidths (especially around specific working wavelength values, such as 385 nm, with high energy concentration) 97, can be costly. In addition, purchasing additional components, such as laserdrivers, may be necessary, which can further increase fabrication costs. Even so, these drivers can be critical since they regulate the current that passes to the laser; otherwise, the light intensity will not be constant, resulting in uneven light distribution and a higher chance of burning the laser. For comparison, an engraving laser module with a low power output of 1 W and a 405 nm wavelength costs approximately one-tenth of the price of the SM7-365A projector. Nevertheless, more expensive and precise lasers, such as a fiber-coupled laser source, can surpass the projector's price. Some laser models used in DLP bioprinting are a UV laser of 375 nm (MW-UV-375) and a 405nm UV laser with adjustable output power 92,93. An alternative is to use laser diodes, although it may be necessary to combine multiple to achieve the high light intensity values needed ⁹⁸. This poses a problem as it requires large amounts of current, which not all electrical components can withstand, in addition to increasing the number of optical components. Similarly, it also requires a laser diode-driver, either by purchasing it, or to reduce costs, developing in-house. One specific research study portrays the usage of blue laser diodes (445 nm; 3500 mW) as a viable light source alternative 99.

On the other hand, LEDs can be used as a light source for the construction of a DLP bioprinter, wherein the precision of the wavelength range is not as accurate as the aforementioned light sources; nevertheless, this can be compensated by coupling multiple LEDs to supply a higher value of light intensity ^{16,33,70,100–106}. LED light sources are commonly used for manufacturing DLP bioprinters since they do not require in-depth knowledge for maintenance and installation; they are disposable, cheap, have low electrical consumption, and do not give off much heat. A downside of using LEDs is that the intensity profile is not uniform; to fix this problem, lenses, LED modules, and/or reflectors can be utilized ^{107–109}. Examples of LEDs used in DLP bioprinting include LC-L1 UV LED chips and a UV-LED M385LP1-C1, each with a wavelength center around 365 nm and 385 nm, respectively ^{70,103}.

The next type of "light source" analyzed are projectors, which are of particular interest since they facilitate the construction of a DLP bioprinter ^{56,81,110}. One of its most significant advantages is that it already has an integrated DMD, which saves the work of arranging all the optical components. However, the disadvantage of this product is that its price is higher than that of developing the bioprinter with separate individual optical components. Also, the image it projects is only focused at a specific distance (focal length), where the image will be blurred outside of this distance. Some examples of projectors used in DLP bioprinting are PRO4500 optical engine (405 nm) and a commercial Acer P1500 DLP visible-light projector ^{40,84}. Notably, there are also reports of variations being done to projectors. Some examples include a tripteron parallel mechanism ¹¹¹ and multi-projector systems 112. The abovementioned mechanisms are used in tandem with stitching, which increases the print area or resolution. Other works have developed a custom optical system to ensure a homogenous light intensity distribution, coupling that with a moving platform and stitching ¹¹³. Moreover, different types of light sources used in DLP bioprinting, such as fluorescent and incandescent lamps and smartphones, are not as efficient or conventional as the previous ones; nevertheless, they showcase the versatility and flexibility of the DLP bioprinting technique 114,115.

3.2 Digital Micromirror Device

DMD is the core technology of a DLP bioprinter and is responsible for giving its fast printability and high resolution ¹¹⁶. This component works by taking light as an input and reflecting some portion of it onto a projection area, with the desired image(s) (seen in **Fig. 5**). This element is composed of an array of micromirrors mounted over a tilting platform; by generating an electrically induced response, each of these elements can flip into an ON or OFF configuration. Thus, an image can be recreated with each micromirror acting as a pixel ¹¹⁷. Furthermore, it can modulate each projection pixel's intensity by switching fast between ON and OFF states, enabling grayscale projection ¹¹⁸. In the following sections, the three main considerations for selecting a DMD, as well as some general installation guidelines, will be analyzed.

3.2.1 Considerations

There are three main factors to consider when selecting a DMD: reflectance, micromirror amount, and pattern rate. For the reflectance, the micromirrors are made of aluminum with a

special coating, which works with different spectrums based on the wavelength regimen: UV, visible light, and near-infrared (NIR) ^{119,120}. Therefore, the importance of DMD reflectance is that the correct reflectance coating must be chosen to work with the desired wavelength. This can be relatively simple since a DMD is usually labeled by its model and the wavelength range it operates ^{121–123}. This information can also be found in the datasheet, which specifies the wavelength range in which the DMD operates. Next, the micromirror amount determines the projection resolution, which is a key parameter in any DLP bioprinter design; however, as this property increases, so does the price. Therefore, finding the optimal synergy between resolution (i.e., micromirror number) and price is vital, oftentimes determined by application needs. As an example, for simple 3D patterns (such as cubes, cylinders, or symmetric geometric patterns), instead of using a highresolution DMD chip, a lower-resolution DMD chip in conjunction with a lens/microscope objective can be implemented to print with higher resolution ¹²⁴. On the other hand, more complex structures, such as asymmetric patterns, highly detailed constructs, and 3D models with a wide variety of sizes, require increased resolution ^{125,126}. To that end, a DMD chip was employed for micro-stereolithography to achieve features with resolutions as low as 0.6 µm ¹⁵. Notably, using an optical system with such high resolution, i.e., micro-stereolithography can reduce the total projection area. Nevertheless, utilizing the stitching technique (e.g., a moving platform) can increase the total projection area. Lastly, pattern rate controls two variables: the number of different projections that can be made in a determined period and amount of grayscale gradients.

Current DMDs are extremely fast, and for a conventional DLP bioprinter, it is not mandatory to change between images in the order of microseconds; most of the polymerization for a given layer occurs in the order of seconds. Another point to consider when selecting the appropriate pattern rate is the available shades of gray. Current DMDs usually have 8 bits (*i.e.*, 256 states) ¹²⁷, and a respective image rate, which represents how many images can be presented in grayscale format per second. To further expand on this, each micromirror has up to 256 different states from minimum light intensity (0% power) to maximum light intensity (100% power). Switching between states is done by modulating the rate (pattern rate) at which each specific micromirror (or pixel) is flipped between ON and OFF to obtain an 'average' of light intensity over a specified period, similar to the pulse-width modulation (PWM) technique (**Fig. 5**). This number of bits (8 bits) is typically enough; though there are some cases where higher bits of information are needed to process an image ^{128,129}. Digging deeper into grayscale, one of the most important applications

of this technology is grayscale DLP (g-DLP) bioprinting, a form of DLP printing that creates a gray mask over the projection ¹³⁰. Different values in the grayscale can change the crosslinking density, resulting in a change in the mechanical properties of the solid ¹³¹. g-DLP has found a versatile range of applications such as 4D printing, fabrication of graded porous structures, improvement of material toughness, and printing of biomimetic structures ^{130,132–135}. Various DMDs have been used in DLP bioprinting; two examples are: the DLP LightCrafter 9000 and DLP Discovery 4000, both elements are a chipset ^{106,121}. The DLP LightCrafter 9000 has integrated a DLP9000 DMD chip with a micromirror array of 2560×1600, a 247-Hz pattern rate in 8-bit grayscale projection, and a 400-700 nm of wavelength range. On the other hand, the DLP Discovery4100 is a chipset with a port capable of supporting 5 DMD chips (DLP650LNIR, DLP7000, DLP9500, DLP7000UV, and DLP9500UV), 2 in the UV spectrum, 2 in the visible, and 1 in NIR; with a micromirror array that ranges from 1024×768 to 1920×1080; and a pattern rate ranging from 1563 Hz to 4069 Hz in 8-bit grayscale projection.

3.2.2 Installation

This section aims to summarize things to consider when installing a DMD. First, this component requires an electronic card to facilitate communication, *i.e.*, sending images from an interface to the DMD. Some distributors already have an electronic card integrated with their software and communication protocols. The DMD also needs a light source to impact the micromirror array and convert this input energy into an output light with the shape of the desired image. The projection made by a DMD is a series of equally spaced projections of the same image with different light intensities (diffraction orders, **Fig. 5**). This is due to the spacing and microstructure of the mirrors, creating various projections at varying angles. The important thing is to focus on the one with the highest intensity, which is the one that is at a specific angle, typically -12° or 12°, from the face of the DMD (second order of diffraction) and project it onto the vat ¹¹⁸.

3.3 Optical System

A DLP bioprinter has a relatively simple optical design; it comprises a light source, from where the light originates and a DMD that reflects and reshapes the light beam before arriving at the resin vat. However, for several DLP bioprinting setups, more components are at play that help to modulate the output light: collimators, lenses, apertures, and mirrors (**Fig. 5**). A proper use of these

elements can result in a more compact and efficient DLP bioprinter. Notably, the number of optical components and the configuration for the optical system, or arrangement, highly depends on the intended application of the DLP setup. Herein, we explore four optical concepts (collimation, magnification, noise filtering, and redirection) essential for constructing the optical system DLP bioprinter. First is collimating (Fig. 5) a light source, typically LEDs or laser diodes, since lasers are already collimated. Next, by arranging different lens configurations, it is possible to play with the magnification (Fig. 5) of the projection (or rays) at determined key points: DMD impact, aperture, and resin vat. Ideally, when the system is built, unwanted diffraction orders from the DMD are filtered (Fig. 5) using an aperture. Additionally, mirrors (Fig. 5) can be used throughout the system to redirect the light so it emits in a specific direction (bottom-up or top-down) ^{16,91–} 94,100-102. As a side note, other elements, such as cameras and dichroic mirrors, can also be implemented in a DLP bioprinter. Said elements are useful to assess the projection at the region of interest 91,136. Additionally, dichroic mirrors have been used for multi-wavelength pattering, resulting in a continuous DLP printing system ¹³⁷. Lastly, other optical elements, such as diffusers, optical fibers, mounts, posts, and translation stages, to name a few, will not be discussed in this review; these elements can often be conveniently purchased from commercial optics vendors. As a reference for the reader, this is one practical example of an optical system used in a DLP system; therein, the optical elements incorporated are adequately explained ¹¹³.

As previously mentioned, a particular case is the use of projectors since adding lenses to this light source may affect the size of the projection as well as the depth of field (*i.e.*, the range of image sharpness). Usually, the size of a projection is manipulated by adjusting the zoom or the distance between lenses. Different models can interchange various projection lenses, thus, enabling different focal lengths and projection sizes.

3.3.1 Collimation

In DLP bioprinting, it is desired to crosslink a complete layer at the same time uniformly or rather homogeneously. Assuming the light source is a laser diode or LED, it is recommended to collimate the light source, which allows for easier manipulation and control of the light before and after being reflected by the DMD ¹³⁸. Collimated light is a set of light rays that travel parallel along the same direction and spread minimally, thus increasing the uniformness of the light intensity profile during crosslinking. One way to achieve such light propagation is by using a lens primarily

defined by its focal length. For this application, it is recommended to focus only on lenses with a positive focal length (biconvex, plano-convex, and positive meniscus) since they are relatively more straightforward to use and can collimate light sources. Thus, to collimate a light source, a lens is placed at a distance equal to its focal length away from the origin of the light source. However, since a light source does not have a specific place where the origin is located, it is necessary to calibrate the distance between it and the lens. This is done by placing the lens at a distance f (focal length) from the light source and then gradually moving the lens closer or further apart and measuring the evolution of the size of the light rays, or rather, the radius of the light beam as it propagates away from the lens. If it is determined that light rays are growing (*i.e.*, diverging) the further they are displaced from the lens, it is necessary to increase the separation between the light source and the lens. Respectively, if it is noticed that the light rays are converging to a point and spreading after that point, it is necessary to put the light source and lens closer together. As another option, a collimator can be used and sometimes recommends an appropriate light source. Many companies provide collimators for laser diodes, LEDs, and optical fibers.

3.3.2 Magnification

An essential property of collimated light rays is that when a lens enters its path (independent of the distance where it is placed), it will converge at the lens's focal length. This is useful as it allows easy manipulation of the magnification (*i.e.*, the ratio between the input and output widths) of the light rays. If two lenses, with focal lengths fl and f2, are placed in the path of collimated light rays, and the distance between them is fl+f2, the magnification will be f2/fl (4f system). For example, when placing a lens with a focal length (f1) of 50 mm and another lens with a focal length (f2) of 150 mm is placed at (f1+f2) 200 mm of separation, the final magnification of the collimated beam will be 3X (f2/f1) its initial magnification. There are several critical points in the optical workflow where it is necessary to change and know the magnification of the light rays, specifically when they impact the DMD, during noise-filtration, and when they impact the resin vat.

At the first critical point, it can be desired to magnify the collimated light rays that impact the DMD to ensure that the energy is distributed evenly throughout the entire DMD's surface ¹³⁹. The next critical point is when the desired light rays are filtered by the aperture, the better the light rays converge at the aperture, the finer the filtration that can be implemented. Lastly, the light rays (or projections) are emitted onto the resin vat at a desired scale (resolution) determined by the

application need. It is worth noting that by implementing the abovementioned magnification method, the light rays are inverted each time they are magnified. Additionally, instead of using multiple lenses, it is possible to use a single lens. If the objective is to make the light rays' size smaller (i.e., converge), it is required to use a lens with a positive focal length and that the distance between it and the target is less than the focal length ¹²². On the other hand, if it is needed to increase the size of the light rays (i.e., diverge), it is possible to use a lens with a negative focal length (biconcave, plano-concave, negative meniscus) or use a positive focal length lens at a distance greater than twice its focal length from the target 108. The rate of change between the distance from the lens to the target and the magnification is equal to the focal length (f) of the lens used, which means that if a magnification (M) is needed, it is necessary to set the lens at a distance $(1-M)\times f$ away from the target. Note that when using a lens with a positive focal length, the projection will be inverted after the focal distance, meaning that the magnification should be considered negative. Another technique to magnify the light rays is to use elements such as projection lenses, as well as microscope objectives, which already have the lenses built in such a way that they create a fixed magnification ¹²⁴. For a more in-depth discussion of the mathematical description for lenses and how to use them to obtain a desired magnification, the reader is referred to other works ¹⁴⁰. Lenses and various optical materials, such as microscope objectives, are available from numerous distributors.

3.3.3 Noise-filtering

To avoid unwanted interaction between the unfiltered light and the bioink, it is recommended to eliminate the various diffraction orders emitted by the DMD chip. One method to do this is by converging the light rays into a point using a lens; if the light rays are collimated, the converging point will be at a focal length (*f*) away from the lens. Ideally only the desired order of diffraction should pass through, which, if the DMD is correctly positioned, will be located at the center of the propagation. Therefore, a filter (aperture) can be placed at the distance where the desired light rays converge (emitted from the desired projection angle) in such a way that only leaves a central opening, thus filtering unwanted light rays ¹⁴¹.

3.3.4 Redirection

For a DLP bioprinter, it is necessary to direct the light rays into a vertical position, either top-to-bottom or bottom-to-top. This can be achieved by reflecting the light using the DMD, which acts as a mirror with an angular offset. There are three approaches to accomplish this: i) with light emanating parallel to the ground, the angle of the DMD can be varied with respect to the ground 105 ; ii) having the DMD parallel to the ground and varying the angle from the light source 122 ; or iii) a combination of both 142 . Furthermore, mirrors can be added to divert light properly and have a more compact bioprinter. Mirrors are simple to use, as they follow the law of reflection, which states that incident light will be reflected by the same angle it impacts the mirror, relative to the perpendicular of its surface. In the case of DMD, it is essential to consider that the projection will be reflected by an extra $\pm 12^{\circ}$ (or the angles specified by the DMD).

Considerations must be taken before purchasing a mirror, mainly coating material and size. To select these properties correctly, it must be consistent with the spectrum of light used (UV, visible, or NIR); the reflectance wavelength range of the mirror should be in the domain of the light source, ensuring that the percentage is above 80%. The mirror's radius should be chosen to encompass the magnified incoming light rays. Metal-coated mirrors are recommended since they are cheap and have good reflectance over a wide range of wavelengths. The most versatile option is the aluminum-coated mirror because it performs adequately for most wavelengths used in DLP bioprinting. On the other hand, silver- and gold-coated mirrors have better reflectance for wavelengths belonging to the visible and NIR ranges. However, they are not recommended for applications that work with UV and, in the case of gold, with blue light. If the light source belongs to the mid-UV range (wavelengths from 200 nm to 300 nm), a special aluminum coating, known as UV enhancement, can be used. Conversely, for wavelengths belonging to the mid-infrared range (wavelengths from 3 to 8 μ m), a special coating for gold mirrors is suggested, known as mid-infrared enhancement. Different suppliers of these various mirrors are readily available.

4 ELECTRONICS

The validation of electrical parameters for the various components implemented in a DLP bioprinter is vital to ensure efficient and reliable printability. The main electronic elements are as follows: an actuator for mechanical movement, a position-sensor, a controller, and a power source. A chart depicting some of the most common electrical components can be seen in **Fig. 6A**.

Mechanical movement helps to displace the stage and, in the case of multi-material, move the additional components (vats and stage, and flow of diverse bioinks, among others) ^{143,144}; usually, this is operated through a motor in conjunction with the motor-driver. The next critical component is the position-sensor, which helps automate the bioprinting process. Furthermore, the controller aids the synchronization of the actuator(s), sensor, and optics, and in some cases, establishes communication with the user and bioprinter through an interface. Lastly, the power source gives the necessary voltage and current to all the aforementioned components. The interconnectivity between these components is depicted in **Fig. 6B** and **C**. In the following sections, these components will be explored in further detail, evaluating the main criteria to consider when designing the electronics system. Specialized electronic components, such as electrical bands for thermal vats, will not be discussed for simplification purposes.

4.1 Mechanical Movement

In this section, the actuator, *i.e.*, the motor, used in various works for the motion of the stage, will be analyzed. The advantages and disadvantages of the motors chosen in previous works will be evaluated according to the resolution and power. It is worth mentioning that the motors typically require an additional component, a motor-driver, to enable the communication between the actuator and controller for the modulation of speed and direction; therefore, some general selection guidelines for this element will also be overviewed.

4.1.1 Motors

The stage must (generally) be able to speed up, slow down, and stop for each layer when desiring high precision and resolution for complex print models ¹⁴⁵; therefore, high precision in alignment and rigidity is necessary for the Z-axis ¹⁴⁶; consequently, it is important to have proper motor selection criteria (**Fig. 6B** and **C**). The primary consideration is the resolution of the motor, which assists with the repeatability of the printing process. Other factors are the torque, especially when printing heavy objects, and the working voltage and current capacity. A standard motor series often used in diverse bioprinters is the NEMA series due to its resolution, torque, low power consumption, and easy control, among other factors ^{147–150}. This series is a practical stepper motor classified by its dimensional parameters, wherein different subclasses exist, such as: hybrid (ideal for low holding torques with a low voltage consumption ¹⁵¹) and bipolar (requires fewer

connections than a unipolar model). Some bioprinting systems utilizing this class select the NEMA 17 series, allowing a medium torque (0.2-0.6 Nm) and moderate resolution while requiring only 12-24 V ^{33,73,150,152,153}. If more torsion is needed, for example, 1 Nm of torque, NEMA 23 may be implemented ⁶¹. Lastly, NEMA 11 has also been used to maintain a compact structure for the Z-axis with a smaller actuator ¹⁸ since it gives an excellent trade-off between footprint (being smaller than the 17 series) and torque; however, the torque capacity, and therefore the maximum weight of the printed structure, will be lower. Other examples have opted for the application of specialized motors, these being: servo motors or direct-current motors for greater ease of control and lower power requirements ¹¹¹; bipolar motors with low power consumption and included mechanical structure ²⁹; or motors for large load weights with a greater number of coils ¹⁵⁴. Also, some of these specialized motors can update a feedback trajectory according to the current movement of the system and the desired printing resolution ¹⁵⁵. Notably, for DLP bioprinting applications the constructs usually have small weights, therefore high torque is typically not needed; however, if micro-sized features are required, then ensuring high resolution and potentially a feedback mechanism could be of use.

4.1.2 Motor-drivers

A stepper driver (**Fig. 6B** and **C**) is a processor chip that acts as a mediator between a stepper motor and the controller; enabling the motor to change directions and modulate its speed without overheating the actuator. General motor drivers have a few standard options based on the voltage required for the selected motor. The A4988 driver allows the operation of bipolar stepper motors from 8-35 V for 1-2 A and up to 1/16 microstep mode ^{70,156–158}. Another is the DRV8825/DRV8824 driver that supports voltages up to 45 V, peak currents of 2.2 A, and up to 1/32 microstep mode ¹⁴⁸. Both examples are commonly used through shields designed to implement many motors, such as the RepRap Arduino Mega Pololu Shield (RAMPS) 1.4 ^{73,150,159,160}. A crucial consideration for both drivers is a low equivalent series resistance (ESR) ceramic capacitor on the chip; therefore, it is recommended to apply decoupling capacitors close to the motor-driver. On the other hand, if a specialized motor is used, a particular driver should be selected, such as the TMC2130 series ¹⁴⁹ or TDC 001 series ^{161,162} with a fixed panel connector. To avoid overheating the stepper motors, the microstepping capabilities of digital microstep drivers, essentially: DM542T drivers ¹⁶³ and

DM422C series ²⁸, have the function of over-voltage and short circuit protection. Also, the SMCI 33 (Nanotec) ¹⁵⁵ series can reduce the current supplied or enable accurate positioning.

4.2 Position-Sensor

The purpose of position, or limit, sensors is to detect the presence of an object at a specific point and feed this event, *via* an output signal, back to the controller (**Fig. 6B** and **C**) to control the mechanical motion ¹⁵⁸. Based on their signal-processing characteristics, this section will discuss the functionality of two commonly used sensor types: limit-switches and optical sensors.

4.2.1 Limit-switch

The most basic sensor consists of a mechanical switch which, when acted by an external force, will change the state of the internal connection and, therefore, the state of the output voltage ⁷³. In turn, switching this output voltage to a high state (3.3 or 5 V) or low state (ground), will be relevant based on the microcontroller used because of the logic applied voltages, which should be almost equal. Furthermore, a programmable child configuration in the sensor ¹¹⁵ should be implemented to automate the system through the microcontroller. Several commercial modules may be implemented to work as this sensor, as well as the most fundamental components, *e.g.*, a normally open or closed mechanical switch, so long as the closed-loop control for the motor can be achieved ^{21,28,44,115}.

4.2.2 Optic sensor

Instead of a mechanical switch, the optical sensor, *i.e.*, photoelectric sensor, consists of a non-visible-light diode and a light-receiver ⁷³. In this way, when the continuous reception of light from the emitter to the receiver is interrupted due to the obstruction of an object, a change in the output signal will be reflected. Then, the principal function of this sensor is equal to a limit-switch where the power supply of the sensor is essential to reflect a sufficient logic voltage for the controller to receive an input signal correctly.

4.3 Controller

The selection of a controller or integrated circuit will depend on the number of drivers, sensors, and optical components implemented in the system. Depending on the application, a cost-effective

option with sufficient memory space and processing speed should be chosen according to the printing needs or the chosen user interface (**Fig. 6B** and **C**). This component can oversee the control, monitoring, management, and other functions of the bioprinter ¹⁶⁴.

4.3.1 Controller requirements

Since the concept of moving the stage in the Z-axis is similar to that of a 3D extrusion bioprinter's Z-axis, a common controller can be sufficient. One example is Arduino-based microcontrollers, which can be selected as bioprinters' controllers due to their affordability, universality 6,148,158, and compatibility with open-source bioprinting software for mechanical control ¹⁶⁵ (Fig. 6B and C). Several examples have opted for 'integrated' controllers and driver configurations, such as RepRap Arduino Mega Polulu Shield (RAMPS)/Arduino board 73,147,148, which can communicate with an interface directly via serial protocol with a 5 V logic voltage. These systems have the advantage of having a larger memory available through the Arduino Mega 2560 115,148,157,160. Otherwise, a Raspberry Pi with a 3.3 V logic voltage has several digital inputs and outputs and specialized connectivity options (e.g., display serial interface (DSI) connector); therefore, it can be used as an interface or to connect with another interface via a high-definition multimedia interface (HDMI) port ¹⁵³ to transmit images ⁷³. Alternatively, depending on the requirements of the bioprinter, a specialized controller can be selected based on the generalpurpose input/output (GPIO) pins, such as LC S7-1215 111 from Siemens or MESA Electronics for an ethernet protocol ¹⁶⁶, to control various input and output signals with an included interface KTP700 touchscreen. Notice that some of these examples are for extrusion bioprinting techniques; however, since the principal objective is to control a motor at a desired value, the control principle is the same for DLP purposes. Careful considerations must be made to ensure that the controller can also project images; if not, an additional component/interface may be needed. Lastly, if more advanced options are required, such as computer-vision tools, then a Raspberry Pi could be utilized due to its camera compatibility. Another alternative is to use a controller with embedded artificial intelligence (AI), such as NVIDIA's Jetson platform, or a LattePanda with integrated Windows capabilities, both of which have multiple GPIO pins for ease of connectivity with other peripherals.

4.4 Power Source

The selection of a power source (**Fig. 6B** and **C**) is directly based on the total current demand and the maximum voltage required for all the electronic components implemented in the system. Although some components can be externally powered using various power sources, many logical elements, such as internal circuits, require a lower logic voltage (5-3.3 V). Hence, there exists the need for a regulation stage to decrease the initial high voltage given by the power source. The following section will present examples of power supplies implemented in various systems.

4.4.1 Current and voltage demand

Several options for power sources are available in the electronics market; still, for optimal performance, it is necessary to look for a model that can deliver enough current load at a constant and stable output voltage (**Fig. 6B** and **C**). As an example, the voltage demand for stepper motors is usually around 12-24 V: the Mean Well RS-15-12 is a 12-V power source, which can deliver a current of 1.3 A ¹⁶⁶ or, for a higher option, a 12 V/5 A power source ^{73,148,160}. Moreover, the selected power source must cover the electrical requirements for the additional components (*i.e.*, light source, DMD, among others).

After selecting a voltage source and ensuring it can provide sufficient current, it is recommended to utilize a low-dropout regulator (LDO) due to its low cost and ease of implementation. This component can provide a lower voltage than the original power source to feed the various components that need a different power voltage; as an example, microcontrollers are energized by a 5 V source ⁷³. Another option is to use multiple external sources ^{73,153}. However, it is essential to maintain a common ground as a standard reference in case those are not entirely isolated systems.

4.5 System efficiency

The efficiency of the electronics for the system is crucial, as low efficiency can lead to overheating, compromising printability and ultimately cell viability. When selecting electronic components, it is essential to choose high-efficiency parts and comprehend their operating temperature range, as specified in their respective datasheet. For instance, NEMA motors typically have an efficiency of over 90% ¹⁶⁷. It is worth noting that the recommended temperature limits for cell viability vary depending on the bioink used, but a general guideline is to avoid exceeding 37

°C for extended periods ¹⁶⁸. Therefore, it is important to locate the electronics, *e.g.*, controller, at a safe distance from the bioprinting area to minimize heat-transfer. This is particularly important in enclosed DLP bioprinters with limited ventilation. Optimal system performance and high cell viability can be achieved by integrating temperature-control systems, humidity-regulation, and CO₂-management, which collectively create an ideal environment for bioprinting ¹⁶⁹.

5 SOFTWARE

Software plays a significant role in a DLP bioprinter's operation, from the voxelization of a computer-aided design (CAD) file to the selection of printing parameters ¹⁷⁰. To understand the importance of DLP software, it is necessary to know all its functions in the 3D bioprinting process. As a general overview, a chart depicting the DLP software workflow is illustrated in **Fig. 7A**. First is the selection of printing parameters; next is the conversion of the input data to output data, usually CAD files to images; last is the synchronization of the projection with the motor movement.

5.1 Printing Parameters

The first step in the software bioprinting workflow is the selection of printing parameters, such as input file selection, exposure time, layer height, multi-material capabilities, and bounce height, among others ¹⁷¹. The exposure time and layer height are relevant because they determine the resolution of the print; the first parameter refers to the time the bioink is exposed to light, and the second to the amount that the stage is displaced ¹⁷². Both parameters are closely related because a longer exposure time to the light source will represent a thicker slice; therefore, a larger layer height would be necessary ¹⁷³. Of note, the selection of exposure time is crucial, as it can significantly impact cell viability, particularly when using high exposure times and UV wavelengths, which can be harmful to cells ⁸⁶. Multi-material capabilities allow the bioprinter to transition smoothly between different bioinks during the printing process, with the switching mechanism determined by the specific hardware configuration. Another parameter to consider is the bounce height, which is determined by the viscosity of the bioink and helps to settle the bioink between layers ⁶.

It is worth mentioning that many of these parameters are interdependent on the bioink selection, wherein the hydrogel, photoinitiator, and photoabsorber can determine the parameters

of the bioprinting process ¹⁷⁴. For this review, bioink considerations and their impact on the software parameters will not be delved into; nevertheless, it is important to highlight that it is also essential to consider this for optimal parameter selection.

5.2 Generation of Images

The next step in the software DLP bioprinting workflow is converting a CAD file to projected images. That is to say that each projected layer comes from a 3D mesh that has been deconstructed into 2D images. A standard tessellation language file (STL), which is a common type of CAD file used in voxelization ^{40,56,175}, is a 3D mesh that represents a 3D geometric model¹⁷⁶. Next, it is necessary to voxelize the STL file, which, in a simplified manner, means changing the 3D mesh into "3D pixels". Finally, the 3D pixels are sliced to obtain the images to be projected ¹⁷⁷. This process is further described in depth in the following paragraphs.

5.2.1 STL to voxel

STL files are one of the most common types of files for 3D printing and, consequently, one of the most used in DLP bioprinting ^{114,178}. These types of files approximate a 3D surface into a triangular mesh ¹⁷⁹. On the other hand, a voxel is the graphical representation of data converted into a 3D pixel; therefore, voxelization consists of converting a discrete 3D surface into a grid of 3D pixels (**Fig. 7B**) ¹⁸⁰. The most common geometry representation for a 3D pixel is a cube; nevertheless, it is not the only one, and it could be represented with more complex geometries, such as interlocking cubes or even spheres, depending on the application ^{181,182}.

There are different algorithms to voxelize an STL based on the requirements and programming language ^{183–186}. The implementation of the voxelization algorithm is limited by the processing capacity since the central processing unit (CPU) plays a vital role in making calculations. This restricts the complexity of algorithms that can be employed. Today, many voxelization algorithms exist, which are easy to implement and are already programmed in languages such as: C, C++, Python, LabView, and MATLAB ^{187–190}. Some examples are: obj2voxels, an open-source library programmed in C++ and with the ability to voxelize STL files by adjusting the resolution; 3D voxelizer, an open-source library for MATLAB where it is possible to voxelize Object (OBJ) files, which is another type of CAD file, and the resolution can be changed; finally, PyVoxelizer, programmed in Python, wherein STL and OBJ can both be used as input files. The differences are

focused on the input CAD file and the programming language as well as the different algorithms employed to voxelize the CAD models. A more in-depth analysis of different voxelization algorithms can be found in **Table 2**.

5.2.2 Voxel to image

Since DLP inherently requires 2D images to be projected onto a resin vat, it is necessary for the voxelized model, a 3D pixel map, to be converted to a series of 2D pixels or images (Fig. 7B) ¹⁸². There are several established algorithms to obtain the contour of voxels. For instance, standard marching squares is one of the most widely used algorithms, which takes the voxels on the perimeter of the layer and draws a line around them. However, a drawback of this algorithm, as opposed to more advanced algorithms, is that it does not consider resolution. Alternatively, multilevel marching squares (MLMS) operates similarly, but incorporates voxels from the next level to predict a more accurate contour ¹⁹¹. Notably, each voxel has a dimension/height, which does not always represent the desired layer height; for which a convolution filter can help to group the voxels, keeping the most relevant information and thus creating the desired number of images and layer height ^{192,193}. There are existing programs that are integrated with STL voxelizers, offering a consolidated solution. Some examples are: PyVoxSurf, an open-source Python library that offers a range of features, including voxelization, STL file slicing, and adjustable resolution and bounds (min/max); PrusaSlice, an open-source library programmed in C++, offers robust slicing capabilities to slice STL and OBJ files, and since the version 2.6, it is possible to add supports; finally, slice stl create path is an open-source library for MATLAB where STL files are used as input. The main differences between these programs are the programming language, the input CAD file, the user interface, a couple of adjustment parameters, and the convolution filters applied to generate the images. A more comprehensive list of different slicers can be found in Table 2.

5.3 Synchronization

The last step in the bioprinting software workflow is the projection and movement of the motor (**Fig. 7B**). The software specifies the duration of the projected images, *i.e.*, exposure time, and the exact movements required to achieve the desired layer height, including the travel distance and activation of these movements. Obtaining the synchronicity of these two aspects is crucial for a

print to be successful. There are some examples where these parameters take a slightly different twist; for example, in CLIP, the movement of the stage and the exposure of the light source is constant and continuous, which allows for faster printing ⁴⁹. Moreover, any additional components that are added to the bioprinter (thermal elements, additional motors and sensors, bioink-injection pumps, and cameras, to name a few) must also be synchronized and automated accordingly.

5.3.1 Projection

The programs used to control a light source are highly dependent on the type of devices used. Although some manufacturers recommend closed-source software, there are open-source alternatives that could help. For example, some projectors used in low-cost DLP bioprinters could use proprietary software, or instead, alternatives such as NanoDLP or LittleRP. These software packages aid in the image-generation from an STL, to the control of the image projection ^{194,195}. To develop a custom 'projection' software from scratch, (typically) it would need to handle the second screen, and some open-source libraries could help, *e.g.*, OpenCV and PyQt5 for Python or Psychtoolbox for MATLAB ¹⁹⁶. Furthermore, incorporating multiple light sources or having a moving light source results in a larger print area due to the stitching of images to create one homogeneous final image. Suppose that the slicing is also optimized to work with the stitching-projection mechanisms; in that case, this can lead to the creation of images where the pixel intensities (of the stitched images) are generated in such a way that the light distribution is homogeneous throughout the entire layer during crosslinking ^{111,112}. Stitching and projecting images must have multiple components working in harmony: software (new slicing algorithm), optics (adjust light intensity values), and electronics (more motors/components).

5.3.2 Interface

The software, or programming language, varies according to the selected interface. If a personal computer is selected as the primary interface, it could work with macOS, Windows, or Linux; based on this, the programming language libraries will only work with the corresponding CPU architecture. Moreover, the computer lacks the capability to directly control external components like motors, necessitating the use of a dedicated controller, such as Arduino, to regulate actuator signals and sensor inputs. Meanwhile, the personal computer will process and display the images and communicate (or synchronize) with the controller, *e.g.*, *via* serial

communication, to coordinate the activation of the diverse signals ¹⁵². On the other hand, if a Raspberry Pi is selected as the interface, it is not necessary to have an extra controller because it has GPIO pins, which could help process signals to and from the actuator and the sensor ¹⁹⁷.

5.4 Open-source software

Currently, some open-source programs make it much simpler (from a software perspective) to develop a DLP bioprinter. These packages can process input parameters, generate images by slicing STL files, project, and achieve synchronicity with the controller. Some examples are: NanoDLP, a slicing software that can be used to control actuators with the help of a controller board ¹⁹⁸; Creation Workshop, a software used for slicing and controlling actuators ^{160,199}; B9 Creator, with tools similar to those mentioned above ²⁰⁰; and custom-made programs in LabView, offering the ability to have a user-friendly interface for parameter-control with the help of a Python slicer ^{201,202}. The main difference among these is the ability to control actuators; while in NanoDLP, there are prefabricated electronic shields for motor control, the other software alternatives must be adapted to the specifications of the bioprinter. On the other hand, B9 Creator has an additional paid professional license, where the capabilities of the software are extended, such as dimensional fine-tuning and material-development support. These software programs are easy to implement on both a computer and advanced controllers, *e.g.*, Raspberry Pi, but first, it is necessary to determine the hardware components of the bioprinter to ensure efficient software development.

Although a 'bootstrap' approach for developing a DLP bioprinter's software is important and often valuable, open-source software can help small laboratories start bioprinting research. This type of software is typically sufficient for most bio-applications, specific tasks or developments are sometimes required. Since these software options are open-source, they have the flexibility to be easily modified and adapted to fit application needs (see **Table 2** for the recompilation).

6 MATERIAL CONSIDERATIONS

In bioprinting, biomaterial hydrogels are often used as extracellular matrix (ECM)-like matrices to provide structural and functional support for the residing cells. Vat-photopolymerization bioprinting relies on material solidification by photo-triggered crosslinking reactions in the presence of photoinitiators ⁸⁶. Therefore, the typical components of the bioink for

DLP bioprinting consist of photo-sensitive hydrogel-precursors, photoinitiators, and photoabsorbers. In addition to cytocompatibility and bioactivity, rheological properties, especially viscosity and gelation speed, are the major considerations of bioink design for DLP bioprinting. High bioink viscosity (>1 Pa.s) will reduce the efficacy of the bioink renewal and impact the printing quality. Regarding gelation, photo-induced free-radical polymerization is a common gelatin mechanism for DLP bioprinting ^{12,86,102,203}. To this end, various vinyl-based hydrophilic precursors and photoinitiators activated by different wavelengths of light have been developed. Photoinitiators with absorption peaks at near-UV to visible light are preferred for bioprinting to minimize the hazards to living cells. Acyl phosphine oxide salt photoinitiators (absorption peak: ~385 nm), such as lithium phenyl (2,4,6-trimethylbenzoyl) phosphinate (LAP), are extensively used ²⁰³. Furthermore, tris(2,2'-bipyridyl)dichloro-ruthenium(II) hexahydrate with sodium persulfate (Ru/SPS) is another photoinitiator that has gained popularity since it is characterized by having an absorption peak in the visible-light spectrum; making it more benign to cells than UV ⁸⁶. It should be noted that the peak absorption of the photoinitiator should match the light source to maximize the gelation rate.

For hydrogel-precursors, (methyl)acrylate and (methyl)acrylamide depravities of synthetic and natural polymers are widely exploited in DLP bioprinting ¹⁰². Among synthetic polymers, polyethylene glycol (PEG), exhibiting non-cytotoxicity and minimal immunogenicity, has been approved by the United States Food and Drug Administration (FDA) for certain biomedical applications. PEG can be tailored with different chain lengths and different architectures, such as linear or multi-armed structures, and modified with different functional groups, such as thiol, vinyl, acetylene, and (methyl)acrylate for different photocrosslinking 204. For example, by altering the polymer concentration and oligomer chain length, PEG-diacrylate (PEGDA) hydrogels with broadly tunable physical properties can be obtained ^{205,206}. However, PEG hydrogels are nonbiodegradable and have inherently poor adhesion to cells or proteins. To this end, biologically active components, such as cell-adhesive peptides (e.g., Arg-Gly-Asp-Ser (RGDS)), growth factor-sequestering heparan sulfate proteins, and matrix metalloproteinases can be incorporated in PEG hydrogels ²⁰⁴. By contrast, natural polymers, including proteins and polysaccharides, show good cytocompatibility and cell bioactivity and can be facilely modified with (methyl)acrylate or similar moieties to accommodate photocuring. For example, gelatin-containing cell-adhesive peptide sequences and protease-sensitive sites can be grafted with methacrylamide and

methacrylate groups, creating the photocurable gelatin methacryloyl (GelMA) ^{207–209}. GelMA hydrogels can be photocured and bioprinted with tunable mechanical properties depending on the degree of substitution, polymer concentration, photoinitiator concentration, and light irradiation conditions ^{210–212}. Other widely used protein-based biomaterials include collagen ²¹³, silk ^{107,214}, decellularized extracellular matrix ²¹⁵, and polysaccharide-based biomaterials, such as alginate ²¹⁶ and hyaluronic acid ^{217,218}, among many others, have been modified for DLP bioprinting. However, natural polymers usually exhibit inferior physical properties compared to native ECM counterparts. Therefore, the multicomponent biomaterials design has become a significant trend to balance mechanical properties and biological performance and improve printability ^{219–221}. **Fig. 8** schematically illustrates the above-mentioned material considerations for DLP bioprinting. For additional information on bioinks used for DLP and other bioprinting, the reader is referred to additional extensive reviews ^{12,23,31,222–224}.

7 DIY SYSTEM CONSIDERATIONS

While the fundamental design considerations necessary for developing a DLP bioprinter have been analyzed, integrating these components into a cohesive, functional system remains crucial. This section provides specific insights into assembling these elements for a DiY DLP bioprinter. Additionally, maintenance tips and basic troubleshooting considerations will be provided to assist readers in ensuring the optimal functionality of their bioprinting setup.

A significant advantage of creating DiY systems lies in their inherent capacity for customization based on specific application needs ²²⁵. Whether it involves modifying the hardware for multi-material applications, integrating a customized optical system with dual-wavelength properties, incorporating advanced electronic systems with embedded AI capabilities, designing a unique slicer with g-DLP properties, or tailoring new materials with specific biomechanical properties, the freedom to customize each feature as needed is invaluable. For a more in-depth analysis of DiY bioprinters, including their history and a comprehensive examination of various examples, readers are referred to our previous review article on the topic ⁶.

7.1 DiY development

The first step in developing these devices is to select the configuration, which could be either bottom-up or top-down. This choice is not just a technical decision, but one that is influenced by

the properties of the bioink the user plans to use and the specific application needs. The choice of configuration also dictates modifications to the hardware, influencing the design and material selections of the vat and stage. For multi-material applications, this choice further necessitates alterations in the vat design.

Subsequently, the choice of configuration dictates the direction of light emittance, which in turn influences the layout and positioning of the optical system. Optical components, such as light source and DMD, should be defined. Various lenses can be positioned to achieve different magnifications: one covering the entirety of the DMD's surface, another for noise filtering, and additional lenses as needed for the desired resolution, coinciding with the vat's window size. For those less familiar with optics, purchasing a projector is recommended to simplify this setup.

With the hardware and optical system established, appropriate electronics, including actuators for the Z-axis and systems to regulate input and output signals, ensuring correct voltage and current distribution, should be integrated. These electronics must also support robust communication with the interface to allow adjustments of printing parameters. Furthermore, software development is crucial for slicing the input CAD file into 2D images, controlling their projection, and synchronization with other components such as motors and sensors.

DiY bioprinters are typically designed for specific applications, closely linked to the properties of the bioink used. Therefore, before developing a DLP bioprinter, users must fully understand their bioink specifications, inclusive of photoinitiators and photoabsorbers, to ensure compatibility with the rest of the design. For more detailed discussions on the implementation of each component (hardware, optics, electronics, software, and materials), readers are directed to the respective sections.

7.2 DiY maintenance

Understanding the fundamentals for the development of DiY bioprinters is crucial, as is knowing how to properly maintain their components, including hardware, optics, electronics, and software. Maintenance of a bioprinter involves a comprehensive approach. Hardware maintenance involves routine checks, replacements, and calibrations to ensure the stage is level and aligned with the vat, and that the Z-axis is greased for smooth movement. Moreover, it is important to check that the film is appropriately tensioned and transparent in bottom-up configurations. Optics maintenance includes regular alignment checks and cleaning of mirrors and lenses to ensure

optimal performance. While electronics may involve inspecting for faulty connections or replacing cost-effective boards that could fail over time. Although software may not require maintenance, it should be regularly updated to enhance functionality and include new features.

Customized bioprinters can face various challenges, including user error, wear-and-tear, or unforeseen issues. Properly identifying the root cause is essential, though often complex. For example, if prints continuously detach, this could indicate a leveling issue with the stage or degradation of the vat's film, necessitating its replacement. If the Z-axis motor malfunctions without recent software changes, the problem could stem from faulty electronics or the motor itself. To diagnose, connecting a new motor to the existing electronics could reveal whether the issue lies with the motor or requires a deeper electronic examination using tools such as multimeters and oscilloscopes.

Additional common issues include burnt-out LEDs in the light source that require replacement or misalignment in the optical system that needs recalibration. In the realm of software, bugs can disrupt functionality; however, these are typically rectifiable through continuous updates. Addressing these problems systematically ensures that the bioprinter maintains its functionality and continues to operate efficiently.

8 FUTURE OUTLOOK

As technological advances continue to develop, there are numerous future opportunities for the creation of 3D constructs using DLP bioprinters ^{226–228}. These technological advances will be prominent in one (or more) of the following subdivisions: stage and resin vat, optics, electronics, software, and materials. Ultimately, these advances can help to improve the resolution and complexity of the bioprinted constructs, leading to a better capability of recreating complex tissues and organs. It is imperative to achieve higher complexity to fabricate different types of human-based models, ranging from brain, liver, heart, lung, muscle, and kidney, among others ^{125,229–233}. Pushing bioprinting to clinical applicability for the creation of complex tissues and organs is the end goal, and to achieve this, technological advances must continue to happen ²³⁴.

One key technology we identify with the potential to greatly influence the resolution and widespread use of DLP bioprinting is AI and machine learning (ML). ML has been implemented in various fields of technology, including additive manufacturing ^{235,236}. In additive biomanufacturing, ML can expedite multiple aspects of the bioprinting workflow, such as

improving the quality of the bioprinted objects. To achieve this, different ML algorithms are employed; convolutional neural networks (CNNs) are an ML subdivision where specific models can be applied (i.e., ResNet) to achieve specific tasks such as image (pixel data) computation and processing in an efficient manner. In a specific additive manufacturing-related example, different CNN architectures models (3D-CNN and CNN-LSTM) were applied for quality detection and printing optimization via printing parameter-correction (feed rate) ^{227,228}. In the context of DLP. ML (ML-DLP) has demonstrated the potential to enhance resolution by scattering correction and analyzing grayscale distribution; the former being utilized for drug release (time) testing and the latter in g-DLP ^{237–239}. Furthermore, a study demonstrated how ML models, Random Forest (RF), could enhance error prediction capabilities influenced by different printing parameters such as light intensity, exposure time, and layer thickness ²⁴⁰. From an optics perspective, ML-DLP can be used with a dichroic mirror and a feedback system for real-time inspection and correction of 3D constructs ^{227,241}. This is further coupled by advanced electronics controllers being developed with embedded AI/ML capabilities, such as NVIDIA's Jetson controller board. Additionally, ML-DLP has shown the potential to predict cell viability with different variables, such as projection parameters or bioink solutions ²⁴². ML shows the capability to improve the bioprinting process and control quality by *in-situ* monitoring.

For the remaining sub-divisions (hardware: stage and resin vat, optics, and electronics), various key technological advances exist that can profoundly aid the progress of DLP bioprinting. As an example, stage and resin vat are a subdivision of great intrigue and continuous development. Recently, several profound contributions have been made to this subdivision, whether developing novel designs that transform bioprinting by enabling multi-material, high(er)-speed, high(er)-resolution, and high(er) complexity. Furthermore, from an optics perspective, commercial solutions by companies have increased the DMD's resolution, achieving pixel amounts as high as 4K or, in some cases, even 8K. Moreover, there has been a development of commercially available 4K DLP projectors capable of emitting dual wavelengths at the same time. This increased resolution and multiple wavelength projection will influence the complexity of constructs that can be printed. Lastly, in electronics, controllers with increased processing capabilities are under development.

The interplay and interconnection of the subdivisions discussed above are crucial to truly push DLP towards becoming a key technology for creating complex tissue constructs. Many of the

turning points in DLP bioprinting have come from developments made in research laboratories. Moreover, the advancements made by researchers from academia and industry will continue to push the boundaries of DLP bioprinting.

9 ACKNOWLEDGMENTS

The support from the National Institutes of Health (R01EB028143, R01HL165176, R01HL166522, R01CA282451, R21HL168656), National Science Foundation (CBET-EBMS-1936105, CISE-IIS-2225698), and Chan Zuckerberg Initiative (2022-316712) is acknowledged.

10 AUTHOR DECLARATIONS

COI (conflict of interest): YSZ consulted for Allevi by 3D Systems, and sits on the scientific advisory board and holds options of Xellar, neither of which however, participated in or bias the work. The interests are managed by the Brigham and Women's Hospital. The other authors declare no COI.

Ethics approval statement: Not applicable.

Author contributions:

Carlos Ezio Garciamendez-Mijares: Conceptualization (lead); supervision (equal); project administration (lead), writing-original draft (equal); writing-review and editing (lead). Francisco Javier Aguilar: Methodology (lead); writing-original draft (lead); writing-review and editing (equal); visualization (lead). Pavel Hernandez: Writing-original draft (equal); visualization (equal). Xiao Kuang: Writing-original draft (equal); writing-review and editing (equal); supervision (supporting). Mauricio Gonzalez: Writing-original draft (equal). Vanessa Ortiz: Writing-original draft (equal). Ricardo A. Riesgo: Writing-original draft (equal). David S. Rendon: Visualization (equal). Victoria Abril Manjarrez Rivera: Methodology (supporting). Juan Carlos Rodriguez: Writing-original draft (supporting). Francisco Lugo Mestre: writing-review (equal). Penelope Ceron Castillo: Visualization (supporting). Abraham Perez: Methodology (supporting). Lourdes Monserrat Cruz: Methodology (supporting). Khoon S. Lim: Writing-review and editing (supporting). Yu Shrike Zhang: Conceptualization (equal); supervision (lead); writing-review and editing (equal); funding acquisition (lead); visualization (supporting).

11 DATA AVAILABILITY

Data availability is not applicable.

12 REFERENCES

- 1. Wohlers, T. & Gornet, T. History of Additive Manufacturing. Wohlers report, 24, (2014).
- 2. Ngo, T. D., Kashani, A., Imbalzano, G., Nguyen, K. T. Q. & Hui, D. Additive manufacturing (3D printing): A review of materials, methods, applications and challenges. *Compos B Eng* **143**, 172–196 (2018).
- 3. Ligon, S. C., Liska, R., Stampfl, J., Gurr, M. & Mülhaupt, R. Polymers for 3D Printing and Customized Additive Manufacturing. *Chem Rev* **117**, 10212–10290 (2017).
- 4. Murphy, S. V. & Atala, A. 3D bioprinting of tissues and organs. *Nat Biotechnol* **32**, 773–785 (2014).
- 5. Murphy, S. V., De Coppi, P. & Atala, A. Opportunities and challenges of translational 3D bioprinting. *Nat Biomed Eng* **4**, 370–380 (2020).
- 6. Garciamendez-Mijares, C. E., Agrawal, P., García Martínez, G., Cervantes Juarez, E. & Zhang, Y. S. State-of-art affordable bioprinters: A guide for the DiY community. *Appl Phys Rev* **8**, (2021).
- 7. Groll, J. *et al.* A definition of bioinks and their distinction from biomaterial inks. *Biofabrication* **11**, (2019).
- 8. Lind, J. U. *et al.* Instrumented cardiac microphysiological devices via multimaterial three-dimensional printing. *Nat Mater* **16**, 303–308 (2017).
- 9. Tang, G. *et al.* Liquid-embedded (bio)printing of alginate-free, standalone, ultrafine, and ultrathin-walled cannular structures. *Proc Natl Acad Sci U S A* **120**, (2023).
- 10. Luo, Z. *et al.* Vertical Extrusion Cryo(bio)printing for Anisotropic Tissue Manufacturing. *Advanced Materials* **34**, (2022).
- 11. Ahrens, J. H. *et al.* Programming Cellular Alignment in Engineered Cardiac Tissue via Bioprinting Anisotropic Organ Building Blocks. *Advanced Materials* **34**, (2022).
- 12. Levato, R. et al. Light-based vat-polymerization bioprinting. *Nature Reviews Methods Primers* **3**, 47 (2023).

- 13. Vanaei, S., Parizi, M. S., Vanaei, S., Salemizadehparizi, F. & Vanaei, H. R. An Overview on Materials and Techniques in 3D Bioprinting Toward Biomedical Application. *Engineered Regeneration* **2**, 1–18 (2021).
- 14. Ke, D., Niu, C. & Yang, X. Evolution of 3D bioprinting-from the perspectives of bioprinting companies. *Bioprinting* **25**, (2022).
- 15. Sun, C., Fang, N., Wu, D. M. & Zhang, X. Projection micro-stereolithography using digital micro-mirror dynamic mask. *Sens Actuators A Phys* **121**, 113–120 (2005).
- 16. Ma, X. *et al.* Deterministically patterned biomimetic human iPSC-derived hepatic model via rapid 3D bioprinting. *Proc Natl Acad Sci U S A* **113**, 2206–2211 (2016).
- 17. Mao, Q. *et al.* Fabrication of liver microtissue with liver decellularized extracellular matrix (dECM) bioink by digital light processing (DLP) bioprinting. *Materials Science and Engineering C* **109**, (2020).
- 18. Grigoryan, B. *et al.* Multivascular networks and functional intravascular topologies within biocompatible hydrogels. *Science* (1979) **364**, 458–464 (2019).
- 19. Rajput, M., Mondal, P., Yadav, P. & Chatterjee, K. Light-based 3D bioprinting of bone tissue scaffolds with tunable mechanical properties and architecture from photocurable silk fibroin. *Int J Biol Macromol* **202**, 644–656 (2022).
- 20. Anandakrishnan, N. *et al.* Fast Stereolithography Printing of Large-Scale Biocompatible Hydrogel Models. *Adv Healthc Mater* **10**, (2021).
- 21. Wang, J.-C., Ruilova, M. & Hsun Lin, Y. The Development of an Active Separation Method for Bottom-Up Stereolithography System* T. *EEE/SICE International Symposium on System Integration (SII)*) 108–114 (2017).
- 22. Santoliquidoa, O., Colombob, P. & Ortonaa, A. Additive Manufacturing of ceramic components by Digital Light Processing: A comparison between the "bottom-up" and the "top-down" approaches. *J Eur Ceram Soc* **39**, 2140–2148 (2019).
- 23. Li, W. *et al.* Recent Advances in Formulating and Processing Biomaterial Inks for Vat Polymerization-Based 3D Printing. *Adv Healthc Mater* **9**, (2020).
- 24. Zhang, Y. et al. Continuous 3D printing from one single droplet. Nat Commun 11, (2020).
- 25. Weber, P. *et al.* Microfluidic bubble-generator enables digital light processing 3D printing of porous structures. *Aggregate* (2023) doi:10.1002/agt2.409.

- 26. Ye, H., Das, S. & Zhou, C. Investigation of separation force for bottom-up stereolithography process from mechanics perspective. *International Design Engineering Technical Conferences and Computers and Information in Engineering Conference* **57045**, V01AT02A030 (2015).
- 27. Choi, J. W. *et al.* Sequential process optimization for a digital light processing system to minimize trial and error. *Sci Rep* **12**, (2022).
- 28. Jiang, T. *et al.* Enhanced Adhesion—Efficient Demolding Integration DLP 3D Printing Device. *Applied Sciences (Switzerland)* **12**, (2022).
- 29. He, H., Xu, J., Yu, X. & Pan, Y. Effect of Constrained Surface Texturing on Separation Force in Projection Stereolithography. *Journal of Manufacturing Science and Engineering, Transactions of the ASME* **140**, (2018).
- 30. Zhao, Z., Tian, X. & Song, X. Engineering materials with light: Recent progress in digital light processing based 3D printing. *Journal of Materials Chemistry C* vol. 8 13896–13917 Preprint at https://doi.org/10.1039/d0tc03548c (2020).
- 31. Ng, W. L. *et al.* Vat polymerization-based bioprinting process, materials, applications and regulatory challenges. *Biofabrication* **12**, (2020).
- 32. Liravi, F., Das, S. & Zhou, C. Separation force analysis and prediction based on cohesive element model for constrained-surface Stereolithography processes. *CAD Computer Aided Design* **69**, 134–142 (2015).
- 33. You, S. *et al.* High cell density and high-resolution 3D bioprinting for fabricating vascularized tissues. *Sci Adv* **9(8)**, (2023).
- 34. Shanjani, Y., Pan, C. C., Elomaa, L. & Yang, Y. A novel bioprinting method and system for forming hybrid tissue engineering constructs. *Biofabrication* 7, (2015).
- 35. Grigoryan, B. *et al.* Development, characterization, and applications of multi-material stereolithography bioprinting. *Sci Rep* **11**, (2021).
- 36. Lipkowitz, G. *et al.* Injection continuous liquid interface production of 3D objects. *Sci Adv*8, 3917 (2022).
- 37. Arcaute, K., Mann, B. K. & Wicker, R. B. Stereolithography of three-dimensional bioactive poly(ethylene glycol) constructs with encapsulated cells. *Ann Biomed Eng* **34**, 1429–1441 (2006).

- 38. Wu, Y., Su, H., Li, M. & Xing, H. Digital light processing-based multi-material bioprinting: Processes, applications, and perspectives. *J Biomed Mater Res A* 11, 527–542 (2023).
- 39. Hong, H. *et al.* Digital light processing 3D printed silk fibroin hydrogel for cartilage tissue engineering. *Biomaterials* **232**, (2020).
- 40. Wang, M. *et al.* Molecularly cleavable bioinks facilitate high-performance digital light processing-based bioprinting of functional volumetric soft tissues. *Nat Commun* **13**, (2022).
- 41. Fritschen, A. *et al.* Investigation and comparison of resin materials in transparent DLP-printing for application in cell culture and organs-on-a-chip. *Biomater Sci* **10**, 1981–1994 (2022).
- 42. Ma, X. *et al.* 3D printed micro-scale force gauge arrays to improve human cardiac tissue maturation and enable high throughput drug testing. *Acta Biomater* **95**, 319–327 (2019).
- 43. Huang, J., Ware, H. O. T., Hai, R., Shao, G. & Sun, C. Conformal Geometry and Multimaterial Additive Manufacturing through Freeform Transformation of Building Layers (SI). *Advanced Materials* **33**, (2021).
- 44. Yi, R., Wu, C., Liu, Y. J., He, Y. & Wang, C. C. L. Delta DLP 3-D Printing of Large Models. *IEEE Transactions on Automation Science and Engineering* **15**, 1193–1204 (2018).
- 45. Peng, X. *et al.* Integrating digital light processing with direct ink writing for hybrid 3D printing of functional structures and devices. *Addit Manuf* **40**, (2021).
- 46. Zhang, Y. S. et al. 3D extrusion bioprinting. Nature Reviews Methods Primers 1, (2021).
- 47. Huang, Y. M. & Jiang, C. P. On-line force monitoring of platform ascending rapid prototyping system. *J Mater Process Technol* **159**, 257–264 (2005).
- 48. Zhou, C., Chen, Y., Yang, Z. & Khoshnevis, B. Development of a multi-material mask-image-projection-based stereolithography for the fabrication of digital materials. *2011 International Solid Freeform Fabrication Symposium* (2011).
- 49. Tumbleston, J. R. *et al.* Continuous liquid interface production of 3D objects. *Science* (1979) **347**, 1349–1352 (2015).
- 50. Lin, Y. S., Chen, M. H. & Yang, C. J. A simultaneously sensing system to improve efficiency of Digital Light Process Printing. *2017 International Conference on Applied System Innovation (ICASI)* **IEEE**, 1379–1382 (2017).

- 51. Yogesh, P., Richa, P., Chandrashekhar, N. S. & Karunakaran, K. P. Layer separation mechanisms in DLP 3D Printing. *Advances in Additive Manufacturing and Joining: Proceedings of AIMTDR 2018* 179–187 (2019).
- 52. Wu, L. *et al.* Bioinspired ultra-low adhesive energy interface for continuous 3D printing: Reducing curing induced adhesion. *Research* **2018**, (2018).
- 53. Jiang, Y., Wang, Y., He, H., Feinerman, A. & Pan, Y. Constrained Window Design in Projection Stereolithography for Continuous Three-Dimensional Printing. *3D Print Addit Manuf* 7, 163–169 (2020).
- 54. Yayue, P., Zhou, Y. & Chen, C. A fast mask projection stereolithography process for fabricating digital models in minutes. *J Manuf Sci Eng* **134**, (2012).
- 55. Zhou, C., Chen, Y., Yang, Z. & Khoshnevis, B. Digital material fabrication using mask-image-projection-based stereolithography. *Rapid Prototyp J* **19**, 153–165 (2013).
- 56. Wang, M. *et al.* Digital Light Processing Based Bioprinting with Composable Gradients. *Advanced Materials* **34**, (2022).
- 57. Kowsari, K., Lee, W., Yoo, S. S. & Fang, N. X. Scalable visible light 3D printing and bioprinting using an organic light-emitting diode microdisplay. *iScience* **24**, (2021).
- 58. Li, Y. *et al.* Theoretical prediction and experimental validation of the digital light processing (DLP) working curve for photocurable materials. *Addit Manuf* **37**, (2021).
- 59. Gritsenko, D. *et al.* On characterization of separation force for resin replenishment enhancement in 3D printing. *Addit Manuf* **17**, 151–156 (2017).
- 60. Kunwar, P., Xiong, Z., McLoughlin, S. T. & Soman, P. Oxygen-Permeable Films for Continuous Additive, Subtractive, and Hybrid Additive/Subtractive Manufacturing. *3D Print Addit Manuf* 7, 216–221 (2020).
- 61. Iano, Y., Saotome, O., Kemper, G., de Seixas, A. C., & de Oliveira, G. G. (Eds.). Proceedings of the 6th Brazilian Technology Symposium (BTSym'20). vol. DGBMS (Springer, 2021).
- 62. Fernandes, J. G. *et al.* Study of mixing process of low temperature co-fired ceramics photocurable suspension for digital light processing stereolithography. *Ceram Int* **47**, 15931–15938 (2021).
- 63. Hafkamp, T., Van Baars, G., De Jager, B. & Etman, P. A trade-off analysis of recoating methods for vat photopolymerization of ceramics. *Proceedings of the 28th Annual*

- International Solid Freeform Fabrication Symposium: an Additive Manufacturing Conference 2017 687–711 (2017).
- 64. Li, X. *et al.* Fabrication of porous β-TCP/58S bioglass scaffolds via top-down DLP printing with high solid loading ceramic-resin slurry. *Mater Chem Phys* **267**, (2021).
- 65. Renap, K. & Kruth, J. P. Recoating issues in stereolithography. *Rapid Prototyp J* 1, 4–15 (1995).
- 66. Pérez-Cortez, J. E. *et al.* Low-Cost Light-Based GelMA 3D Bioprinting via Retrofitting: Manufacturability Test and Cell Culture Assessment. *Micromachines (Basel)* **14**, (2023).
- 67. Kuhnt, T., Morgan, F. L. C., Baker, M. B. & Moroni, L. An efficient and easily adjustable heating stage for digital light processing set-ups. *Addit Manuf* **46**, (2021).
- 68. Walker, D. A., Hedrick, J. L. & Mirkin, C. A. Rapid, large-volume, thermally controlled 3D printing using a mobile liquid interface. *Science* (1979) **366**, 360–364 (2019).
- 69. Beh, C. W. *et al.* A fluid-supported 3D hydrogel bioprinting method. *Biomaterials* **276**, (2021).
- 70. Miri, A. K. *et al.* Microfluidics-enabled multimaterial maskless stereolithographic bioprinting. *Advanced Materials* **30**, (2018).
- 71. Choi, J. W., MacDonald, E. & Wicker, R. Multi-material microstereolithography. *International Journal of Advanced Manufacturing Technology* **49**, 543–551 (2010).
- 72. Inamdar, A., Magana, M., Medina, F., Grajeda, Y. & Wicker, R. Development of an automated multiple material stereolithography machine. *International Solid Freeform Fabrication Symposium* (2006).
- 73. Matte, C. D., Pearson, M., Trottier-Cournoyer, F., Dafoe, A. & Kwok, T. H. Automated storage and active cleaning for multi-material digital-light-processing printer. *Rapid Prototyp J* **25**, 864–874 (2019).
- 74. Wicker, R., Medina, F. & Elkins, C. Multiple material micro-fabrication: extending stereolithography to tissue engineering and other novel applications. *International Solid Freeform Fabrication Symposium* (2004).
- 75. Li, Y. et al. Vat Photopolymerization Bioprinting with a Dynamic Support Bath. Addit Manuf 69, (2023).
- 76. Lin, H. *et al.* Application of visible light-based projection stereolithography for live cell-scaffold fabrication with designed architecture. *Biomaterials* **34**, 331–339 (2013).

- 77. Alessandri, K. *et al.* A 3D printed microfluidic device for production of functionalized hydrogel microcapsules for culture and differentiation of human Neuronal Stem Cells (hNSC). *Lab Chip* **16**, 1593–1604 (2016).
- 78. Xue, D., Zhang, J., Wang, Y. & Mei, D. Digital Light Processing-Based 3D Printing of Cell-Seeding Hydrogel Scaffolds with Regionally Varied Stiffness. *ACS Biomater Sci Eng* 5, 4825–4833 (2019).
- 79. González, G. *et al.* Materials testing for the development of biocompatible devices through vat-polymerization 3d printing. *Nanomaterials* **10**, 1–13 (2020).
- 80. Schmidleithner, C. *et al.* Application of high resolution DLP stereolithography for fabrication of tricalcium phosphate scaffolds for bone regeneration. *Biomedical Materials* (*Bristol*) **14**, (2019).
- 81. He, Y. *et al.* A photocurable hybrid chitosan/acrylamide bioink for DLP based 3D bioprinting. *Mater Des* **202**, (2021).
- 82. Sun, Y. *et al.* Modeling the printability of photocuring and strength adjustable hydrogel bioink during projection-based 3D bioprinting. *Biofabrication* **13**, (2021).
- 83. Su, J. J. M., Lin, C. H., Chen, H., Lee, S. Y. & Lin, Y. M. Biofabrication of cell-laden gelatin methacryloyl hydrogels with incorporation of silanized hydroxyapatite by visible light projection. *Polymers (Basel)* **13**, (2021).
- 84. Lim, S. H., Ng, J. Y. & Kang, L. Three-dimensional printing of a microneedle array on personalized curved surfaces for dual-pronged treatment of trigger finger. *Biofabrication* **9**, (2017).
- 85. Shin, C. S. & Chang, Y. C. Fabrication and compressive behavior of a micro-lattice composite by high resolution dlp stereolithography. *Polymers (Basel)* **13**, 1–17 (2021).
- 86. Lim, K. S. *et al.* Fundamentals and Applications of Photo-Cross-Linking in Bioprinting. *Chem Rev* **120**, 10662–10694 (2020).
- 87. Colosi, C. *et al.* Microfluidic Bioprinting of Heterogeneous 3D Tissue Constructs Using Low-Viscosity Bioink. *Advanced Materials* **28**, 677–684a (2016).
- 88. Lim, K. S. *et al.* New Visible-Light Photoinitiating System for Improved Print Fidelity in Gelatin-Based Bioinks. *ACS Biomater Sci Eng* **2**, 1752–1762 (2016).

- 89. Billiet, T., Gevaert, E., De Schryver, T., Cornelissen, M. & Dubruel, P. The 3D printing of gelatin methacrylamide cell-laden tissue-engineered constructs with high cell viability. *Biomaterials* **35**, 49–62 (2014).
- 90. AlShaafi, M. M. Factors affecting polymerization of resin-based composites: A literature review. *Saudi Dental Journal* **29**, 48–58 (2017).
- 91. Kunwar, P. *et al.* High-Resolution 3D Printing of Stretchable Hydrogel Structures Using Optical Projection Lithography. *ACS Appl Mater Interfaces* **12**, 1640–1649 (2020).
- 92. Yang, W. *et al.* Modular and Customized Fabrication of 3D Functional Microgels for Bottom-Up Tissue Engineering and Drug Screening. *Adv Mater Technol* **5**, (2020).
- 93. Yang, W., Yu, H., Liang, W., Wang, Y. & Liu, L. Rapid fabrication of hydrogel microstructures using UV-induced projection printing. *Micromachines (Basel)* **6**, 1903–1913 (2015).
- 94. Skliutas, E. *et al.* A Bio-Based Resin for a Multi-Scale Optical 3D Printing. *Sci Rep* **10**, (2020).
- 95. Valente, F. *et al.* Bioprinting silk fibroin using two-photon lithography enables control over the physico-chemical material properties and cellular response. *Bioprinting* **25**, (2022).
- 96. He, C. & Becker, C. H. Surface Analysis with 1014-1015 W cm-' Laser-Intensities. Surface and Interface Analysis: An International Journal devoted to the development and application of techniques for the analysis of surfaces, interfaces and thin films 24, 79–85 (1996).
- 97. Upputuri, P. K. & Pramanik, M. Fast photoacoustic imaging systems using pulsed laser diodes: a review. *Biomed Eng Lett* **8**, 167–181 (2018).
- 98. Loterie, D., Delrot, P. & Moser, C. High-resolution tomographic volumetric additive manufacturing. *Nat Commun* **11**, (2020).
- 99. Cui, K. J. *et al.* Blue laser diode-initiated photosensitive resins for 3D printing. *J Mater Chem C Mater* **5**, 12035–12038 (2017).
- 100. Martinez, J. S. *et al.* High resolution DLP stereolithography to fabricate biocompatible hydroxyapatite structures that support osteogenesis. *PLoS One* **17**, (2022).
- 101. Ma, X. *et al.* Rapid 3D bioprinting of decellularized extracellular matrix with regionally varied mechanical properties and biomimetic microarchitecture. *Biomaterials* **185**, 310–321 (2018).

- 102. Yu, C. *et al.* Photopolymerizable Biomaterials and Light-Based 3D Printing Strategies for Biomedical Applications. *Chem Rev* **120**, 10695–10743 (2020).
- 103. Xue, D. *et al.* Projection-Based 3D Printing of Cell Patterning Scaffolds with Multiscale Channels. *ACS Appl Mater Interfaces* **10**, 19428–19435 (2018).
- 104. Musgrove, H. B., Catterton, M. A. & Pompano, R. R. Applied tutorial for the design and fabrication of biomicrofluidic devices by resin 3D printing. *Anal Chim Acta* **1209**, (2022).
- 105. Carbonell, C. et al. Polymer brush hypersurface photolithography. Nat Commun 11, (2020).
- 106. Hwang, H. H. *et al.* High throughput direct 3D bioprinting in multiwell plates. *Biofabrication* **13**, (2021).
- 107. Kim, S. H. *et al.* Precisely printable and biocompatible silk fibroin bioink for digital light processing 3D printing. *Nat Commun* **9**, (2018).
- 108. Ma, Y. *et al.* Biomacromolecule-based agent for high-precision light-based 3D hydrogel bioprinting. *Cell Rep Phys Sci* **3**, (2022).
- 109. Chen, C. & Zhang, X. H. Collimate LED light to uniform illumination with refractive-reflective optical system. *Applied Mechanics and Materials* **543–547**, 658–661 (2014).
- 110. Wang, Z. *et al.* A simple and high-resolution stereolithography-based 3D bioprinting system using visible light crosslinkable bioinks. *Biofabrication* 7, (2015).
- 111. Huang, J., Zhang, B., Xiao, J. & Zhang, Q. An Approach to Improve the Resolution of DLP 3D Printing by Parallel Mechanism. *Applied Sciences (Switzerland)* **12**, (2022).
- 112. Wu, L. *et al.* EHMP-DLP: multi-projector DLP with energy homogenization for large-size 3D printing. *Rapid Prototyp J* **24**, 1500–1510 (2018).
- 113. Waldbaur, A., Carneiro, B., Hettich, P., Wilhelm, E. & Rapp, B. E. Computer-aided microfluidics (CAMF): From digital 3D-CAD models to physical structures within a day. *Microfluid Nanofluidics* **15**, 625–635 (2013).
- 114. Melilli, G. *et al.* DLP 3D printing meets lignocellulosic biopolymers: Carboxymethyl cellulose inks for 3D biocompatible hydrogels. *Polymers (Basel)* **12**, (2020).
- 115. Li, W. *et al.* A Smartphone-Enabled Portable Digital Light Processing 3D Printer. *Advanced Materials* **33**, (2021).
- 116. Zhang, J., Hu, Q., Wang, S., Tao, J. & Gou, M. Digital light processing based three-dimensional printing for medical applications. *Int J Bioprint* **6**, 12–27 (2020).

- 117. Wang, Z. *et al.* Digital micro-mirror device-based light curing technology and its biological applications. *Opt Laser Technol* **143**, (2021).
- 118. Yoder, L. A. *et al.* DLP technology: applications in optical networking. *Spatial light modulators: Technology and applications* **4457**, 54–61 (2001).
- 119. Wavelength Transmittance Considerations for DLP ® DMD Window Application Report Wavelength Transmittance Considerations for DLP ® DMD Window. www.ti.com (2012).
- 120. Quijada, M. A. *et al.* Optical evaluation of digital micromirror devices (DMDs) with UV-grade fused silica, sapphire, and magnesium fluoride windows and longterm reflectance of bare devices. *In Advances in Optical and Mechanical Technologies for Telescopes and Instrumentation II* **9912**, 1756–1765 (2016).
- 121. Chen, Y. et al. Noninvasive in vivo 3D bioprinting. Sci Adv 6(23), (2020).
- 122. Zhong, Z. *et al.* Rapid 3D bioprinting of a multicellular model recapitulating pterygium microenvironment. *Biomaterials* **282**, (2022).
- 123. Wang, Z. *et al.* Visible Light Photoinitiation of Cell Adhesive Gelatin Methacryloyl Hydrogels for Stereo-lithography 3D Bioprinting. *ACS Appl Mater Interfaces* **10(32)**, 26859–26869 (2018).
- 124. Lowry Curley, J., Jennings, S. R. & Moore, M. J. Fabrication of micropatterned hydrogels for neural culture systems using dynamic mask projection photolithography. *Journal of Visualized Experiments* (2011) doi:10.3791/2636.
- 125. Mao, Q. *et al.* Fabrication of liver microtissue with liver decellularized extracellular matrix (dECM) bioink by digital light processing (DLP) bioprinting. *Materials Science and Engineering C* **109**, (2020).
- 126. Li, W. *et al.* Stereolithography apparatus and digital light processing-based 3D bioprinting for tissue fabrication. *iScience* **26**, 106039 (2023).
- 127. Dupuis, J. R., Mansur, D. J., Vaillancourt, R., Benedict-Gill, R. & Newbry, S. P. High-dynamic range DMD-based IR scene projector. *Emerging Digital Micromirror Device Based Systems and Applications V* **8618**, 86180R (2013).
- 128. Lowen, J. M. & Leach, J. K. Functionally Graded Biomaterials for Use as Model Systems and Replacement Tissues. *Adv Funct Mater* **30**, (2020).
- 129. Kasi, D. G. et al. Rapid Prototyping of Organ-on-a-Chip Devices Using Maskless Photolithography. *Micromachines (Basel)* **13**, (2022).

- 130. Wu, J. *et al.* Reversible shape change structures by grayscale pattern 4D printing. *Multifunctional Materials* **1**, (2018).
- 131. Montgomery, S. M., Hamel, C. M., Skovran, J. & Qi, H. J. A reaction–diffusion model for grayscale digital light processing 3D printing. *Extreme Mech Lett* **53**, (2022).
- 132. Balakrishnan, H. K. *et al.* 3D Printing Functionally Graded Porous Materials for Simultaneous Fabrication of Dense and Porous Structures in Membrane-Integrated Fluidic Devices. *Small Struct* 2200314 (2023) doi:10.1002/sstr.202200314.
- 133. Leben, L. M., Schwartz, J. J., Boydston, A. J., D'Mello, R. J. & Waas, A. M. Optimized heterogeneous plates with holes using 3D printing via vat photo-polymerization. *Addit Manuf* 24, 210–216 (2018).
- 134. Yue, L. *et al.* Single-vat single-cure grayscale digital light processing 3D printing of materials with large property difference and high stretchability. *Nat Commun* **14**, (2023).
- 135. Kuang, X. *et al.* Grayscale digital light processing 3D printing for highly functionally graded materials. *Sci Adv* **5(5)**, (2019).
- 136. Yoon, J. & Park, W. Microsized 3D Hydrogel Printing System using Microfluidic Maskless Lithography and Single Axis Stepper Motor. *Biochip J* **14**, 317–325 (2020).
- 137. De Beer, M. P. *et al.* Rapid, continuous additive manufacturing by volumetric polymerization inhibition patterning. *Sci Adv* **5(1)**, (2019).
- 138. Dogan, E., Bhusal, A., Cecen, B. & Miri, A. K. 3D Printing metamaterials towards tissue engineering. *Appl Mater Today* **20**, (2020).
- 139. Deng, Q. *et al.* Fabrication of micro-optics elements with arbitrary surface profiles based on one-step maskless grayscale lithography. *Micromachines (Basel)* **8**, (2017).
- 140. Guenther, B. D. & Steel, D. G. Encyclopedia of Modern Optics.
- 141. Zhu, W. *et al.* Direct 3D bioprinting of prevascularized tissue constructs with complex microarchitecture. *Biomaterials* **124**, 106–115 (2017).
- 142. Jiang, G. *et al.* A 3D-printed PRP-GelMA hydrogel promotes osteochondral regeneration through M2 macrophage polarization in a rabbit model. *Acta Biomater* **128**, 150–162 (2021).
- 143. Sampson, K. L. *et al.* Multimaterial Vat Polymerization Additive Manufacturing. *ACS Appl Polym Mater* **3**, 4304–4324 (2021).

- 144. Zhang, Y. F. *et al.* Miniature Pneumatic Actuators for Soft Robots by High-Resolution Multimaterial 3D Printing. *Adv Mater Technol* **4**, (2019).
- 145. Fiedor, P. & Ortyl, J. A new approach to micromachining: High-precision and innovative additive manufacturing solutions based on photopolymerization technology. *Materials* **13**, 1–25 (2020).
- 146. Aristizabal, S. L. *et al.* Microlens array fabricated by a low-cost grayscale lithography maskless system. *Optical Engineering* **52**, 125101 (2013).
- 147. Honiball, J. R., Pepper, M. S. & Prinsloo, E. Step-by-step assembly and testing of a low-cost bioprinting solution for research and educational purposes. *MethodsX* **8**, (2021).
- 148. Saorin, J. L., Diaz-Alemán, M. D., De La Torre-Cantero, J., Meier, C. & Pérez Conesa, I. Design and validation of an open source 3D printer based on digital ultraviolet light processing (DLP), for the improvement of traditional artistic casting techniques for microsculptures. *Applied Sciences (Switzerland)* 11, (2021).
- 149. Koch, F. *et al.* Open-source hybrid 3D-bioprinter for simultaneous printing of thermoplastics and hydrogels. *HardwareX* **10**, (2021).
- 150. Cubo, N., Garcia, M., Del Cañizo, J. F., Velasco, D. & Jorcano, J. L. 3D bioprinting of functional human skin: Production and in vivo analysis. *Biofabrication* **9**, (2017).
- 151. Reid, J. A. *et al.* Accessible bioprinting: Adaptation of a low-cost 3D-printer for precise cell placement and stem cell differentiation. *Biofabrication* **8**, (2016).
- 152. Suryatal, B. K., Sarawade, S. S. & Deshmukh, S. P. Fabrication of medium scale 3D components using stereolithography system for rapid prototyping. *Journal of King Saud University Engineering Sciences* (2021) doi:10.1016/j.jksues.2021.02.012.
- 153. Gupta, P., Bhat, M., Khamkar, V., Tandel, G. & Salunkhe, G. Designing of cost effective resin 3D printer using UV LED. in *2020 International Conference on Convergence to Digital World Quo Vadis, ICCDW 2020* (Institute of Electrical and Electronics Engineers Inc., 2020). doi:10.1109/ICCDW45521.2020.9318691.
- 154. Tesavibul, P. *et al.* Biocompatibility of hydroxyapatite scaffolds processed by lithography-based additive manufacturing. *Biomed Mater Eng* **26**, 31–38 (2015).
- 155. Hatzenbichler, M., Geppert, M., Seemann, R. & Stampfl, J. Additive manufacturing of photopolymers using the Texas Instruments DLP lightcrafter. *Emerging Digital Micromirror Device Based Systems and Applications V* **8618**, 86180A (2013).

- 156. Lee, M. P. *et al.* Development of a 3D printer using scanning projection stereolithography. *Sci Rep* **5**, (2015).
- 157. Nguyen, H. B., Vo, T., Nguyen, T. K. & Hoang, D. L. A Research of Design Controller of 3D Printer DLP Technology. *Applied Mechanics and Materials* **902**, 71–78 (2020).
- 158. Liu, J., Tang, J. L. & Dai, C. Y. Design of DLP 3D printer control system based on arduino.

 *Proceedings 2020 3rd World Conference on Mechanical Engineering and Intelligent Manufacturing, WCMEIM 2020 497–500 (2020) doi:10.1109/WCMEIM52463.2020.00110.
- 159. Lin, Y. S., Lin, Y. Z., Zhang, Y. Y. & Yang, C. J. Simulating an intelligent printing control for a digital light processing (DLP) 3D printer. *2018 IEEE International Conference on Applied System Invention (ICASI)* 429–432 (2018).
- 160. Barone, S., Neri, P., Paoli, A., Razionale, A. V. & Tamburrino, F. Development of a DLP 3D printer for orthodontic applications. *Procedia Manuf* **38**, 1017–1025 (2019).
- 161. Kuang, X. *et al.* High-Speed 3D Printing of High-Performance Thermosetting Polymers via Two-Stage Curing. *Macromol Rapid Commun* **39**, (2018).
- 162. Khairu, K. *et al.* Study on layer fabrication for 3D structure of photoreactive polymer using DLP projector. *Applied Mechanics and Materials* **465–466**, 911–915 (2014).
- 163. Fitzsimmons, R. E. *et al.* Generating vascular channels within hydrogel constructs using an economical open-source 3D bioprinter and thermoreversible gels. *Bioprinting* **9**, 7–18 (2018).
- 164. Deng, W. et al. DLP-Based 3D Printing for Automated Precision Manufacturing. *Mobile Information Systems* **2022**, (2022).
- 165. Lee, J., Kim, K. E., Bang, S., Noh, I. & Lee, C. A desktop multi-material 3D bio-printing system with open-source hardware and software. *International Journal of Precision Engineering and Manufacturing* **18**, 605–612 (2017).
- 166. Fortunato, G. M. *et al.* Robotic platform and path planning algorithm for in situ bioprinting. *Bioprinting* **22**, (2021).
- 167. Keinz, J. R. & Senior, R. L. H. NEMA Nominal Efficiency-What Is It and Why. *IEEE Trans Ind Appl* 454–457 (1981).
- 168. Landers, R. *et al.* Fabrication of soft tissue engineering scaffolds by means of rapid prototyping techniques. *J Mater Sci* **37**, 3107–3116 (2002).

- 169. Matamoros, M. *et al.* Temperature and humidity pid controller for a bioprinter atmospheric enclosure system. *Micromachines (Basel)* **11**, (2020).
- 170. Ma, D., Lin, F. & Chua, C. K. Rapid Prototyping Applications in Medicine. Part 2: STL File Generation and Case Studies. *Int J Adv Manuf Technol* **18**, 118–127 (2001).
- 171. Yang, Y., Zhou, Y., Lin, X., Yang, Q. & Yang, G. Printability of external and internal structures based on digital light processing 3D printing technique. *Pharmaceutics* **12**, (2020).
- 172. He, Y. et al. Research on the printability of hydrogels in 3D bioprinting. Sci Rep 6, (2016).
- 173. Goodarzi Hosseinabadi, H. *et al.* Ink material selection and optical design considerations in DLP 3D printing. *Appl Mater Today* **30**, (2023).
- 174. Torras, N. *et al.* A simple DLP-bioprinting strategy produces cell-laden crypt-villous structures for an advanced 3D gut model. *BioRxiv* (2022) doi:10.1101/2022.02.09.479715.
- 175. Ma, C. *et al.* Photoacoustic imaging of 3D-printed vascular networks. *Biofabrication* **14**, (2022).
- 176. Szilvśi-Nagy, M. & Matyasi, G. Y. Analysis of STL Files. *Math Comput Model* **38(7–9)**, 945–960 (2003).
- 177. Patil, S. & Ravi, B. Voxel-based Representation, Display and Thickness Analysis of Intricate Shapes. *Ninth International Conference on Computer Aided Design and Computer Graphics (CAD-CG'05)* 6-pp (2005).
- 178. Daly, A. C., Prendergast, M. E., Hughes, A. J. & Burdick, J. A. Bioprinting for the Biologist. *Cell* **184**, 18–32 (2021).
- 179. Rypl, D. & Bittnar, Z. Generation of computational surface meshes of STL models. *J Comput Appl Math* **192**, 148–151 (2006).
- 180. Cohen-Or, D. & Kaufman, A. Fundamentals of Surface Voxelization. *Graphical models and image processing* **57(6)**, 453–461 (1995).
- 181. Zhang, Y. & Balkcom, D. Interlocking structure assembly with voxels. *IEEE/RSJ International Conference on Intelligent Robots and Systems (IROS)2016* 2173–2180 (2016).
- 182. Hiller, J. & Lipson, H. Design and analysis of digital materials for physical 3D voxel printing. *Rapid Prototyp J* **15**, 137–149 (2009).

- 183. Schwarz, M. & Seidel, H.-P. Fast Parallel Surface and Solid Voxelization on GPUs. *ACM transactions on graphics (TOG)* **29(6)**, 1–10 (2010).
- 184. Rassineux, A. & Beckers, B. A robust smoothed voxel representation for the generation of finite element models for computational urban physics. *An International Conference on Urban Physics* (2016).
- 185. Wang, S. W. & Kaufman, A. E. Volume Sampled Voxelization of Geometric Primitives. *Proceedings Visualization'93* 78–84 (1993).
- 186. Chen, H. *et al.* Grid refinement in lattice Boltzmann methods based on volumetric formulation. *Physica A: Statistical Mechanics and its Applications* **362**, 158–167 (2006).
- 187. Dong, Z., Chen, W., Bao, H., Zhang, H. & Peng, Q. A Smart Voxelization Algorithm. *Proceedings of Pacific Graphics* 43–50 (2004).
- 188. Lai, X. & Wei, Z. Slicing algorithm and partition scanning strategy for 3d printing based on gpu parallel computing. *Materials* **14**, (2021).
- 189. Mathotaarachchi, S. *et al.* VoxelStats: A MATLAB package for multi-modal voxel-wise brain image analysis. *Front Neuroinform* **10**, (2016).
- 190. Lee, H., Shin, D., Shin, S. & Hyun, J. Effect of gelatin on dimensional stability of silk fibroin hydrogel structures fabricated by digital light processing 3D printing. *Journal of Industrial and Engineering Chemistry* **89**, 119–127 (2020).
- 191. Ghadai, S., Jignasu, A. & Krishnamurthy, A. Direct 3D printing of multi-level voxel models. *Addit Manuf* **40**, (2021).
- 192. Singh, R. D., Mittal, A. & Bhatia, R. K. 3D convolutional neural network for object recognition: a review. *Multimed Tools Appl* **78**, 15951–15995 (2019).
- 193. Yang, J. *et al.* Reinventing 2D Convolutions for 3D Images. *IEEE J Biomed Health Inform* **25**, 3009–3018 (2021).
- 194. Subirada, F. *et al.* Development of a Custom-Made 3D Printing Protocol with Commercial Resins for Manufacturing Microfluidic Devices. *Polymers (Basel)* **14**, (2022).
- 195. Borrello, J., Nasser, P., Iatridis, J. C. & Costa, K. D. 3D printing a mechanically-tunable acrylate resin on a commercial DLP-SLA printer. *Addit Manuf* **23**, 374–380 (2018).
- 196. Zhang, W. *et al.* An Improved Python-Based Image Processing Algorithm for Flotation Foam Analysis. *Minerals* **12**, (2022).

- 197. Yaman, U., Dolen, M., Dilberoglu, U. M. & Gharehpapagh, B. A New Method for Generating Image Projections in DLP-type 3D Printer Systems. *Procedia Manuf* 11, 490–500 (2017).
- 198. Shin, S. H. *et al.* Evaluation of dimensional changes according to aging period and postcuring time of 3d-printed denture base prostheses: An in vitro study. *Materials* **14**, (2021).
- 199. Valentinčič, J., Peroša, M., Jerman, M., Sabotin, I. & Lebar, A. Low cost printer for DLP stereolithography. *Strojniski Vestnik/Journal of Mechanical Engineering* **63**, 559–566 (2017).
- 200. Yaman, U., Dolen, M. & Hoffmann, C. Generation of patterned indentations for additive manufacturing technologies. *IISE Trans* **51**, 209–217 (2019).
- 201. Shin, D. & Hyun, J. Silk fibroin microneedles fabricated by digital light processing 3D printing. *Journal of Industrial and Engineering Chemistry* **95**, 126–133 (2021).
- 202. Zhang, B. *et al.* Mechanically Robust and UV-Curable Shape-Memory Polymers for Digital Light Processing Based 4D Printing. *Advanced Materials* **33**, (2021).
- 203. Lee, M., Rizzo, R., Surman, F. & Zenobi-Wong, M. Guiding Lights: Tissue Bioprinting Using Photoactivated Materials. *Chem Rev* **120**, 10950–11027 (2020).
- 204. Zhu, J. Bioactive modification of poly(ethylene glycol) hydrogels for tissue engineering. *Biomaterials* **31**, 4639–4656 (2010).
- 205. Nguyen, Q. T., Hwang, Y., Chen, A. C., Varghese, S. & Sah, R. L. Cartilage-like mechanical properties of poly (ethylene glycol)-diacrylate hydrogels. *Biomaterials* 33, 6682–6690 (2012).
- 206. Della Sala, F. *et al.* Mechanical behavior of bioactive poly(ethylene glycol) diacrylate matrices for biomedical application. *J Mech Behav Biomed Mater* **110**, (2020).
- 207. Van Den Bulcke, A. I. *et al.* Structural and rheological properties of methacrylamide modified gelatin hydrogels. *Biomacromolecules* **1**, 31–38 (2000).
- 208. Son, T. Il *et al.* Visible light-induced crosslinkable gelatin. *Acta Biomater* **6**, 4005–4010 (2010).
- 209. Yue, K. *et al.* Synthesis, properties, and biomedical applications of gelatin methacryloyl (GelMA) hydrogels. *Biomaterials* **73**, 254–271 (2015).

- 210. Miri, A. K., Hosseinabadi, H. G., Cecen, B., Hassan, S. & Zhang, Y. S. Permeability mapping of gelatin methacryloyl hydrogels. *Acta Biomater* 77, 38–47 (2018).
- 211. Ying, G., Jiang, N., Yu, C. & Zhang, Y. S. Three-dimensional bioprinting of gelatin methacryloyl (GelMA). *Biodes Manuf* 1, 215–224 (2018).
- 212. O'Connell, C. D. *et al.* Tailoring the mechanical properties of gelatin methacryloyl hydrogels through manipulation of the photocrosslinking conditions. *Soft Matter* **14**, 2142–2151 (2018).
- 213. Diamantides, N. *et al.* Correlating rheological properties and printability of collagen bioinks: the effects of riboflavin photocrosslinking and pH. *Biofabrication* **9**, (2017).
- 214. Xie, M. *et al.* Volumetric additive manufacturing of pristine silk-based (bio)inks. *Nat Commun* **14**, (2023).
- 215. Gao, G., Park, J. Y., Kim, B. S., Jang, J. & Cho, D. W. Coaxial Cell Printing of Freestanding, Perfusable, and Functional In Vitro Vascular Models for Recapitulation of Native Vascular Endothelium Pathophysiology. *Adv Healthc Mater* 7, (2018).
- 216. Jeon, O., Bouhadir, K. H., Mansour, J. M. & Alsberg, E. Photocrosslinked alginate hydrogels with tunable biodegradation rates and mechanical properties. *Biomaterials* **30**, 2724–2734 (2009).
- 217. Skardal, A. *et al.* Photocrosslinkable hyaluronan-gelatin hydrogels for two-step bioprinting. *Tissue Eng Part A* **16**, 2675–2685 (2010).
- 218. Skardal, A., Zhang, J. & Prestwich, G. D. Bioprinting vessel-like constructs using hyaluronan hydrogels crosslinked with tetrahedral polyethylene glycol tetracrylates. *Biomaterials* **31**, 6173–6181 (2010).
- 219. Cui, X. *et al.* Advances in Extrusion 3D Bioprinting: A Focus on Multicomponent Hydrogel-Based Bioinks. *Adv Healthc Mater* **9**, (2020).
- 220. Bedell, M. L., Navara, A. M., Du, Y., Zhang, S. & Mikos, A. G. Polymeric Systems for Bioprinting. *Chem Rev* **120**, 10744–10792 (2020).
- 221. Kuang, X., Arıcan, M. O., Zhou, T., Zhao, X. & Zhang, Y. S. Functional Tough Hydrogels: Design, Processing, and Biomedical Applications. *Acc Mater Res* **4**, 101–114 (2023).
- 222. Gungor-Ozkerim, P. S., Inci, I., Zhang, Y. S., Khademhosseini, A. & Dokmeci, M. R. Bioinks for 3D bioprinting: An overview. *Biomater Sci* **6**, 915–946 (2018).
- 223. Decante, G. et al. Engineering bioinks for 3D bioprinting. Biofabrication 13, (2021).

- 224. Khoeini, R. *et al.* Natural and Synthetic Bioinks for 3D Bioprinting. *Adv Nanobiomed Res* 1, (2021).
- 225. Wolf, M. & McQuitty, S. Understanding the do-it-yourself consumer: DIY motivations and outcomes. *AMS Review* **1**, 154–170 (2011).
- 226. Jin, Z., Zhang, Z., Shao, X. & Gu, G. X. Monitoring Anomalies in 3D Bioprinting with Deep Neural Networks. *ACS Biomater Sci Eng* (2021) doi:10.1021/acsbiomaterials.0c01761.
- 227. Lee, X. Y., Saha, S. K., Sarkar, S. & Giera, B. Automated detection of part quality during two-photon lithography via deep learning. *Addit Manuf* **36**, (2020).
- 228. Menon, A., Póczos, B., Feinberg, A. W. & Washburn, N. R. Optimization of Silicone 3D Printing with Hierarchical Machine Learning. *3D Print Addit Manuf* **6**, 181–189 (2019).
- 229. Walus, K., Beyer, S. & Willerth, S. M. Three-dimensional bioprinting healthy and diseased models of the brain tissue using stem cells. *Curr Opin Biomed Eng* **14**, 25–33 (2020).
- 230. Tang, M., Rich, J. N. & Chen, S. Biomaterials and 3D Bioprinting Strategies to Model Glioblastoma and the Blood–Brain Barrier. *Advanced Materials* **33**, (2021).
- 231. Bliley, J. *et al.* FRESH 3D bioprinting a contractile heart tube using human stem cell-derived cardiomyocytes. *Biofabrication* **14**, (2022).
- 232. da Rosa, N. N. *et al.* Three-Dimensional Bioprinting of an In Vitro Lung Model. *Int J Mol Sci* **24**, 5852 (2023).
- 233. Lawlor, K. T. *et al.* Cellular extrusion bioprinting improves kidney organoid reproducibility and conformation. HHS Public Access. *Nat Mater* **20**, 260–271 (2021).
- 234. Bejoy, A. M. *et al.* An insight on advances and applications of 3d bioprinting: A review. *Bioprinting* **24**, (2021).
- 235. Jin, Z., Zhang, Z. & Gu, G. X. Autonomous in-situ correction of fused deposition modeling printers using computer vision and deep learning. *Manuf Lett* **22**, 11–15 (2019).
- 236. Delli, U. & Chang, S. Automated Process Monitoring in 3D Printing Using Supervised Machine Learning. *Procedia Manuf* **26**, 865–870 (2018).
- 237. You, S. *et al.* Mitigating scattering effects in light-based three-dimensional printing using machine learning. *Journal of Manufacturing Science and Engineering, Transactions of the ASME* **142**, (2020).

- 238. Stanojević, G. *et al.* Tailoring Atomoxetine Release Rate from DLP 3D-Printed Tablets Using Artificial Neural Networks: Influence of Tablet Thickness and Drug Loading. *Molecules* **26**, (2021).
- 239. Zhao, B., Zhang, M., Dong, L. & Wang, D. Design of grayscale digital light processing 3D printing block by machine learning and evolutionary algorithm. *Composites Communications* **36**, (2022).
- 240. Wang, X., Liu, J., Dong, R., Gilchrist, M. D. & Zhang, N. High-precision digital light processing (DLP) printing of microstructures for microfluidics applications based on a machine learning approach. *Virtual Phys Prototyp* **19**, (2024).
- 241. Dedeloudi, A., Weaver, E. & Lamprou, D. A. Machine learning in additive manufacturing & Microfluidics for smarter and safer drug delivery systems. *Int J Pharm* **636**, (2023).
- 242. Xu, H. *et al.* Prediction of cell viability in dynamic optical projection stereolithography-based bioprinting using machine learning. *J Intell Manuf* **33**, 995–1005 (2022).

13 TABLES AND FIGURES

Table 1. Comparison of commonly used light sources (including projectors).

Light source	Subclass	Wavelength (nm)	Luminous intensity (lm) / Output power (mW)	Spectral bandwidth (nm)	Cost	Supplier	Resolution
	LBX-405-50-				Mid-		
	CSB-PPA	405	50-300 mW	1.60E-06	High	RPMC	-
					Mid-		
Laser	D40-R	406.4	5-1000 mW	< 0.06	High	Laser Glow	-
Laser					High-	Edmund	
	OBIS LX/LS	405	50-250 mW	4.00E-04	Low	Optics	-
	Cobolt 06-01				High-	Hübner	
	Series	365-1064	25-250 mW	< 2	Low	photonics	-
					Low-		
	PLPT9	447	5000 mW	~2	Low	OSRAM	-
			400, 600, 1000		Low-		
Laser diode	RWLD	405	mW	2	High	RPMC Lasers	-
					Low-		
	NV4V31MF	405	175 mW	~0.4	High	Renesas	-
					Mid-		
	L473P100	473	100 mW	<1	High	ThorLabs	-
LED					Low-		
	UV5TZ	385-405	20, 40 mW	~5	Low	BIVAR	-
	J-Series Color		600, 700, 800		Low-		
	LEDs	450-740	mW	~20	Low	Cree LED	-
	LUXEON UV				Low-		
	U Line	385-415	425-2610 mW	9-13.7	Low	LUMILEDS	-
	UV Mounted				Mid-		
	LEDs	365-405	880-2050 mW	9-12.5	Low	ThorLabs	-
Projector		405,460,525,613	320, 745, 1330	15, 19, 20,	Mid-		
	Pro 4500	and RGB	lm	34	High	Wintech	1280×800

				Low-		
PS600X	white light	3700 lm	-	High	Viewsonic	1024×768
405 DLP				Mid-		
PDC05	405	200-300 lm	-	High	ZS	1920×1080
DLP 4710				Mid-	Texas	
EVM-LC	455, 525, 620	600 lm	21, 27, 33	High	Instruments	1920×1080
				High-		
DLP670S	385, 405	6400 mW	-	High	In-vision	3840×2160

 Table 2. Commonly used software for DLP development.

Name	Specification	Туре	Open-source
3D voxelizer	Library in MATLAB	Voxelizer	Yes
B9 Creator	Package	Voxelizer, slicer, and interface	Yes
Chitubox basic	Package	Voxelizer, slicer, and interface	Yes
Creation Workshop	Package	Voxelizer, slicer, and interface	Yes
Cuda_voxelizer	Library in C++	Voxelizer	Yes
Hackathon-slicer	Library in Java	Slicer	Yes
LittleRP	Package	Voxelizer, slicer, and interface	Yes
Lychee Slicer	Package	Voxelizer, slicer, and interface	Yes
Mesh voxelization	Library in MATLAB	Voxelizer	Yes
Monkeyprint	Package	Voxelizer, slicer, and interface	Yes
NanoDLP	Package	Voxelizer, slicer, and interface	Yes
Obj2voxels	Library in C++	Voxelizer	Yes
Polydat_to_imagedata	Library in Python	Voxelizer	Yes
PrusaSlice	Library in C++	Slicer	Yes
PyVoxelizer	Library in Python	Voxelizer	Yes
PyVoxSurf	Library in Python	Voxelizer and slicer	Yes
Slice_stl_create_path	Library in MATLAB	Slicer	Yes
Stl-to-voxel	Library in Python	Voxelizer	Yes
Allevi Bioprint	Package	Voxelizer, slicer, and interface	No
BuildBee	Package	Voxelizer, slicer, and interface	No
DNA Studio 4	Package	Voxelizer, slicer, and interface	No
Formware 3D	Package	Voxelizer, slicer, and interface	No
GrabCAD Print Pro	Package	Voxelizer, slicer, and interface	No

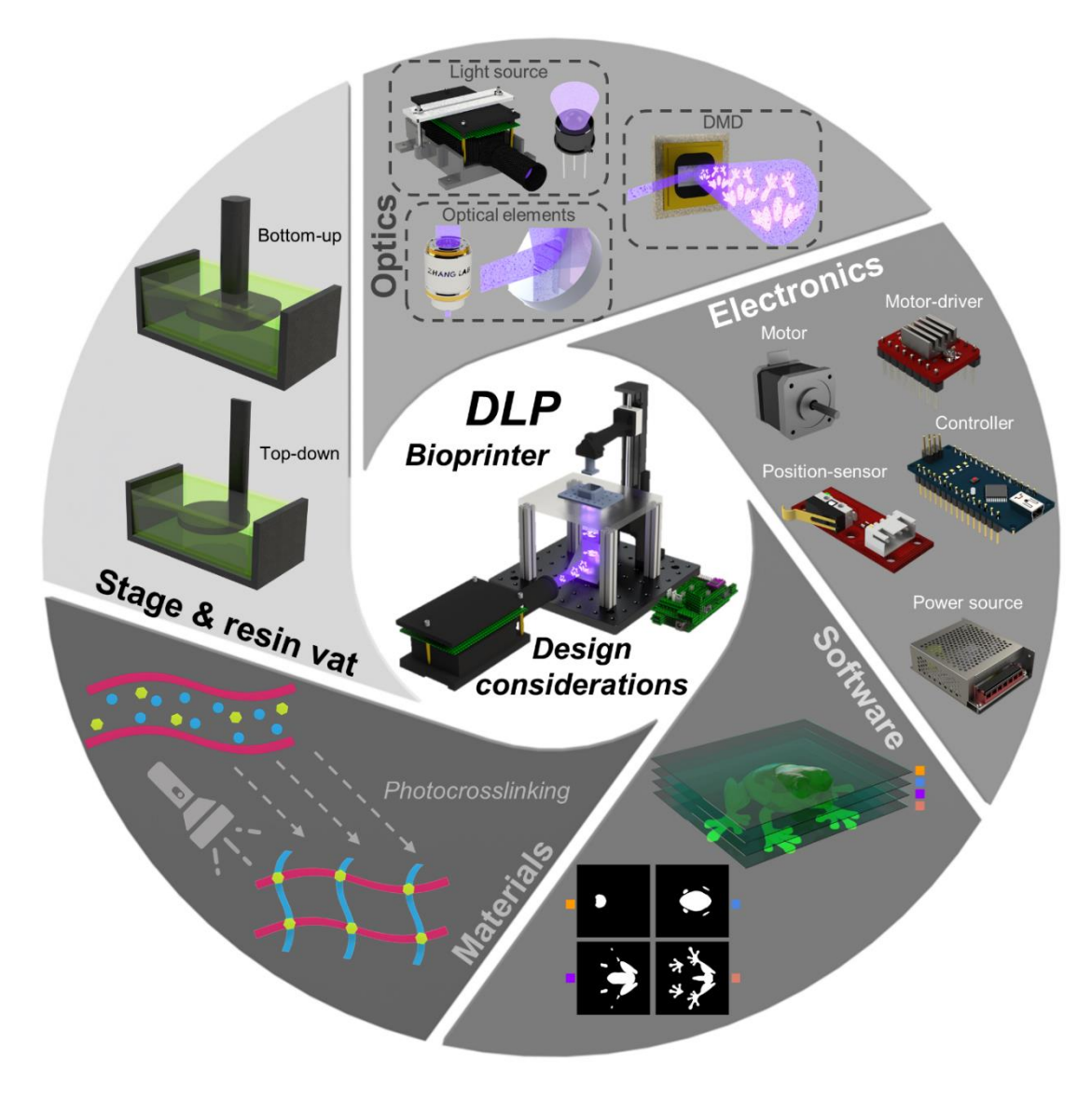


Fig. 1. Overview of DLP bioprinter design considerations.

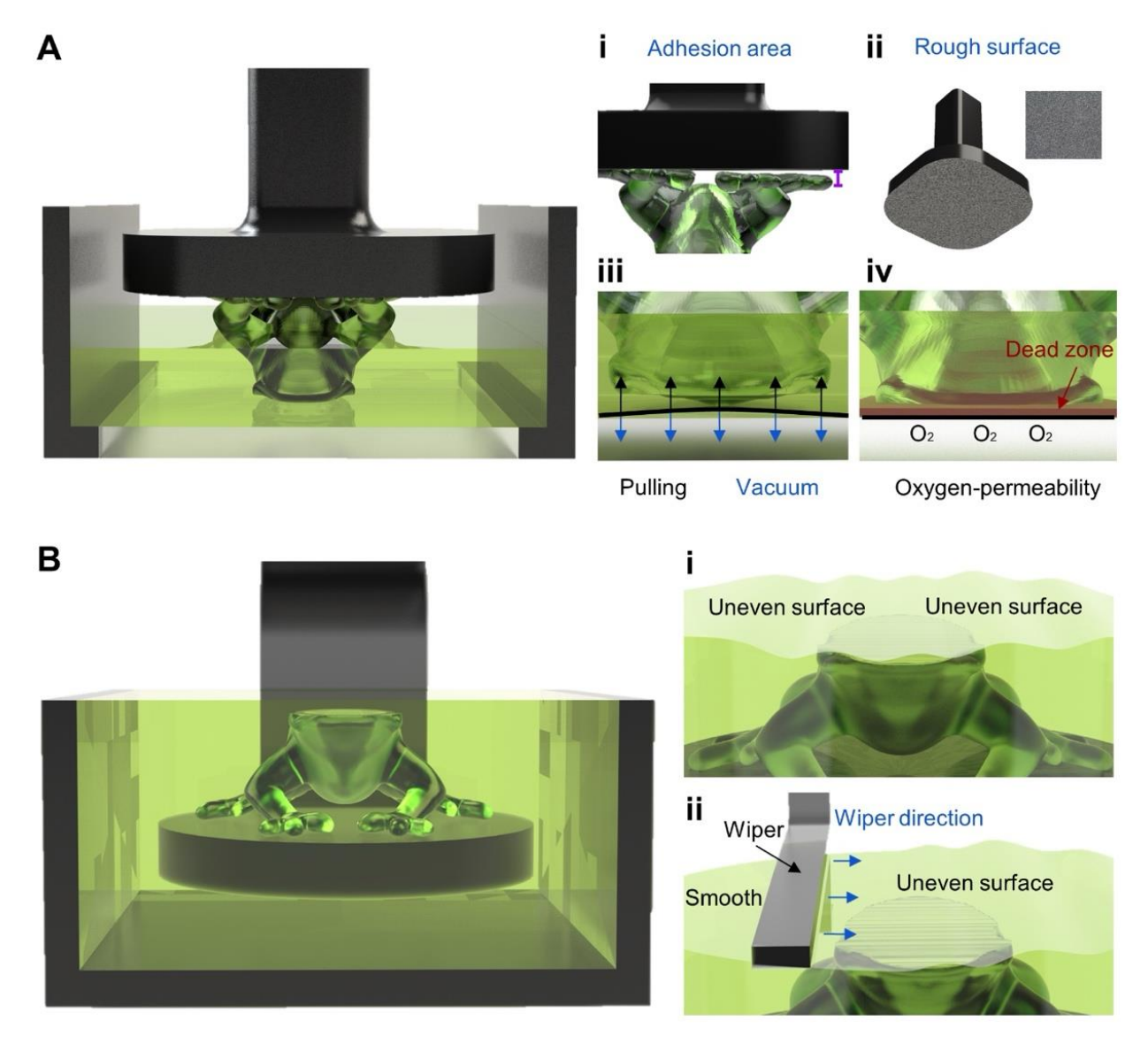


Fig. 2. Stage and vat designs according to configuration. A. Bottom-up configuration: (i) adhesion issue that may occur; (ii) rough surface to promote surface adhesion; (iii) vacuum/suction forces on print and film; (iv) having an oxygen-permeable film enables a dead zone that promotes print separation. **B.** Top-down configuration: (i) inconsistent layer issue that may occur; (ii) implementation of wiper to create homogeneous layer.

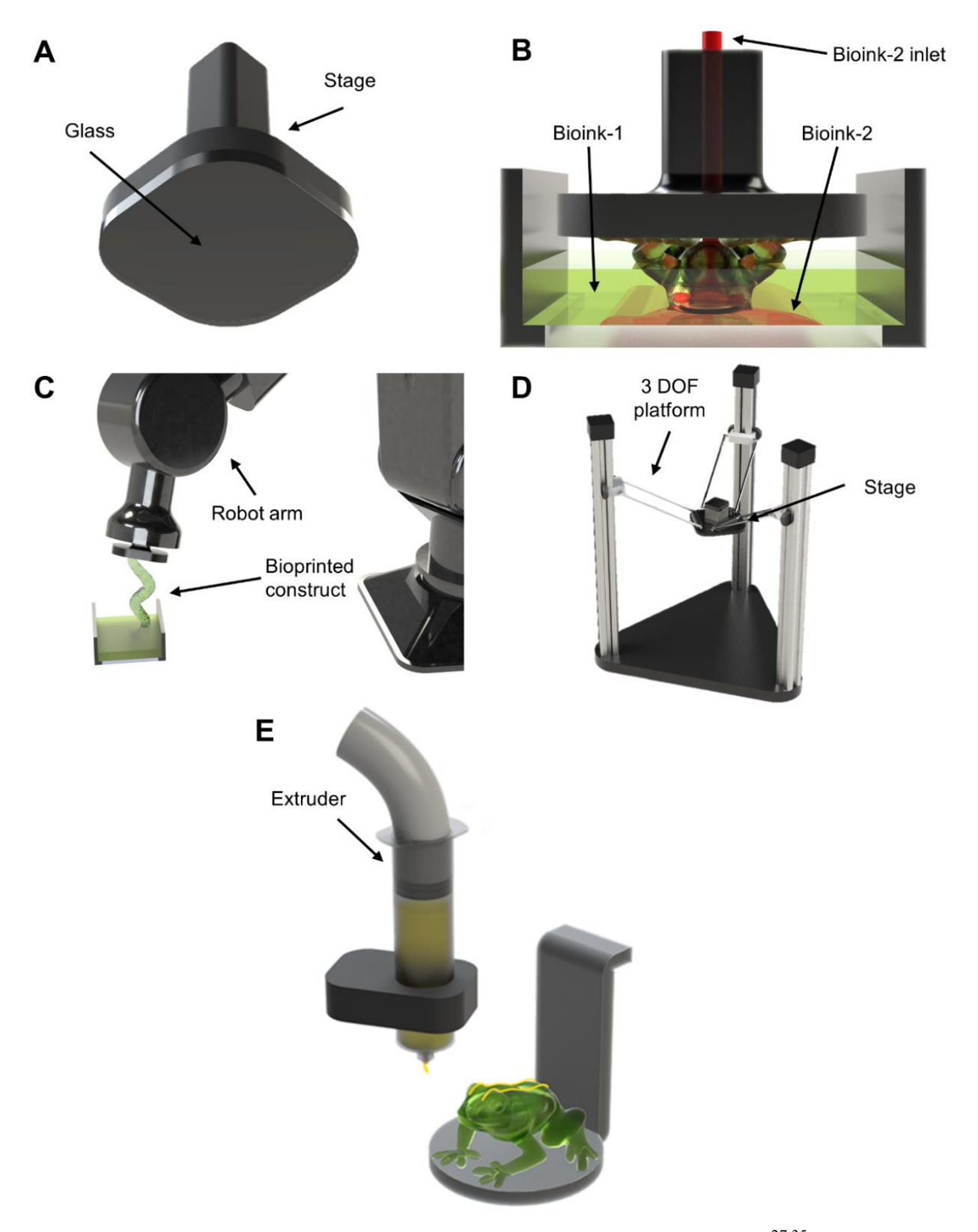


Fig. 3. Specific stage examples. A. Generic stage design using glass surface ^{27,35} for flatness. **B.** iCLIP design ³⁶ of stage with a secondary bioink inlet. **C.** Robotic arm as a stage ⁴³ to create

complex structures without supports. **D.** Delta-mounted stage ⁴⁴ for increased print area and resolution (stitching). **E.** Multi-technique DLP bioprinting with extrusion ⁴⁵ for the fabrication of multi-material constructs.

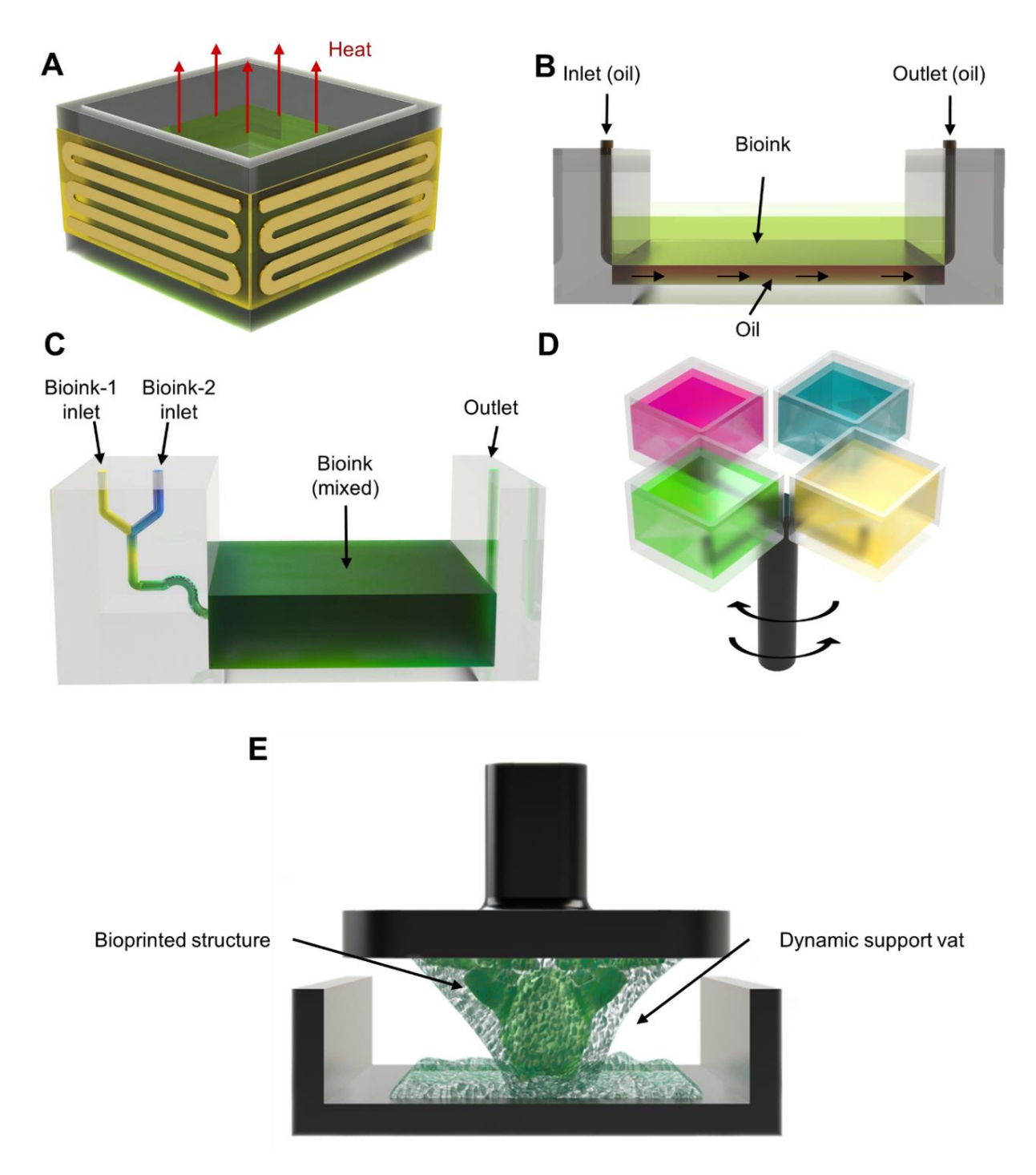


Fig. 4. Specific vat examples. **A.** Generic vat design to control heat to regulate bioink viscosity and for cellular viability. **B.** High area rapid printing (HARP) ⁶⁸. **C.** Microfluidic vat ⁵⁶. **D.** Carousel-inspired top-down multi-vat ⁷². **E.** Dynamic support bath ⁷⁵ incorporated into the vat.

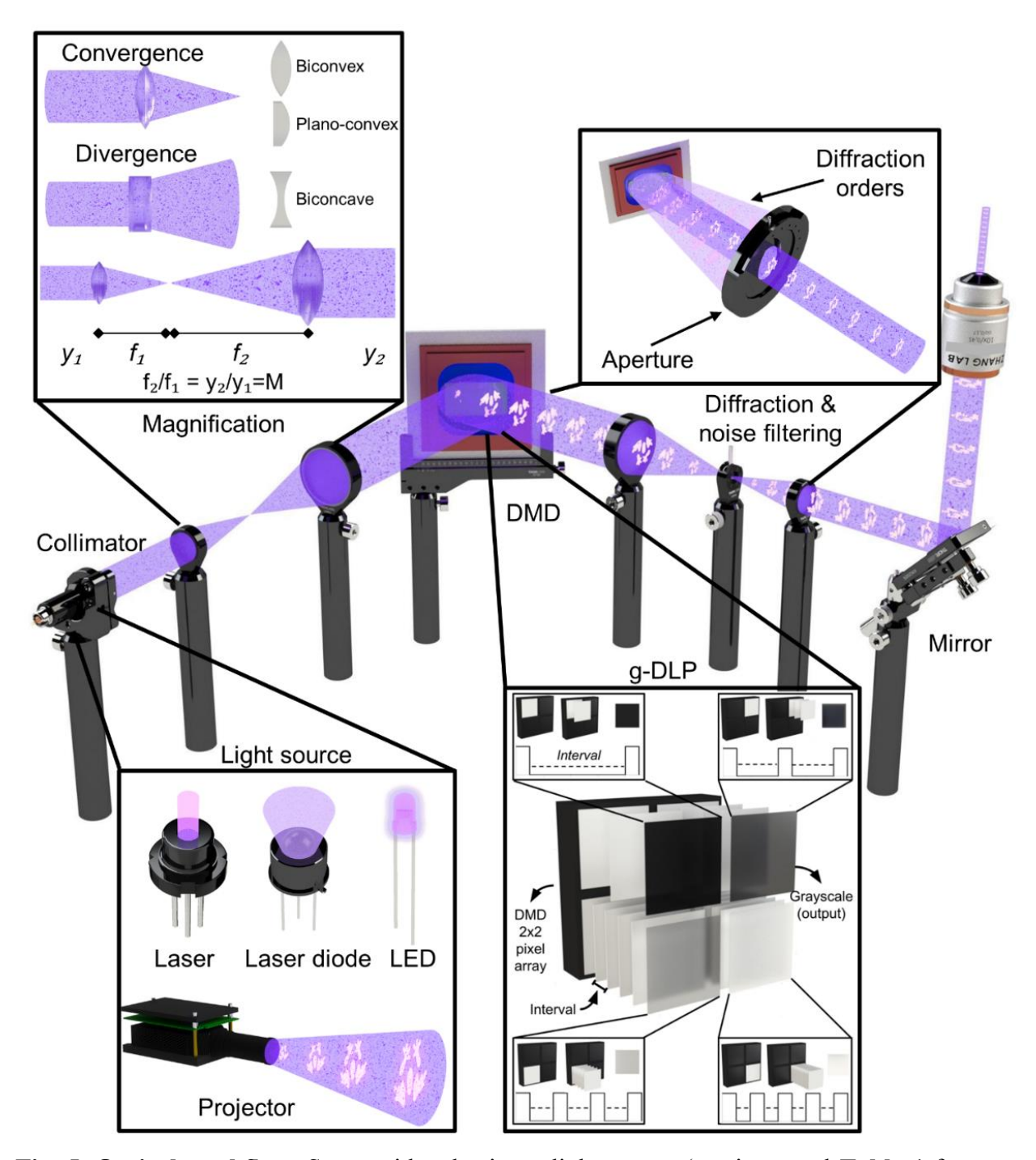


Fig. 5. Optical workflow. Starts with selecting a light source (see inset and **Table 1** for more information); projectors are not considered in this setup. Next, if needed, collimate the light, and play with the magnification until impacting the DMD surface. Also, g-DLP and its functionality in respect to the DMD technology is illustrated; an example a 2×2-pixel array emitting four different tones of grey. Afterward, it is necessary to filter (utilizing lenses and apertures) unwanted diffraction orders. Throughout the setup, mirrors can be used to redirect the light in a particular

direction (*i.e.*, bottom-up *versus* top-down). Lastly, more magnification methods can be utilized, such as a microscope objective, to obtain the projected image to the desired size.

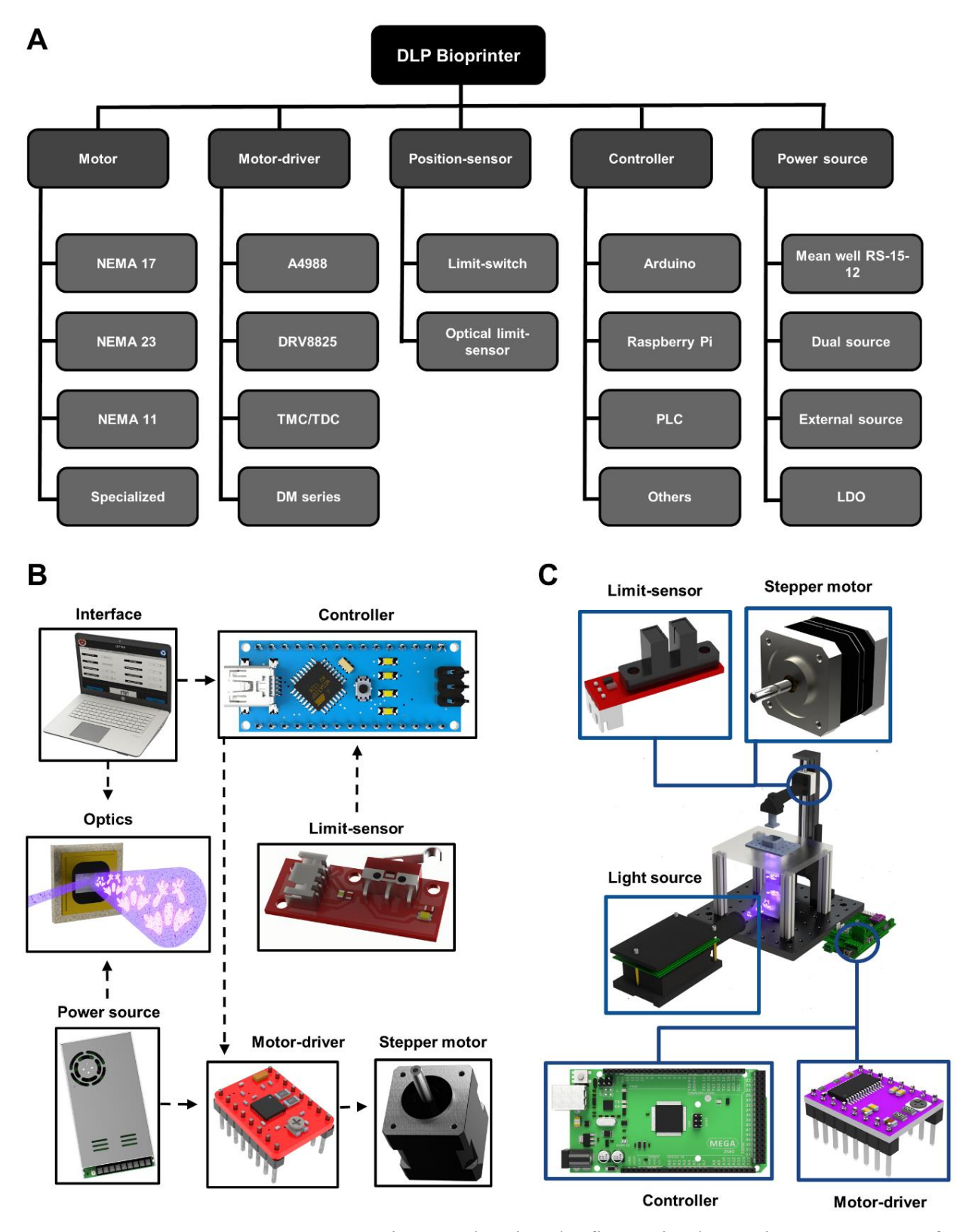


Fig. 6. Electronics components. A. Diagram showing the five main electronics components of a DLP bioprinter (motor, motor-driver, position-sensor, controller, and power source); each category

is then labeled with some pertinent models. **B.** Overview of the connection of main electronic components is provided. **C.** Main electronic layout example in a DLP bioprinter.

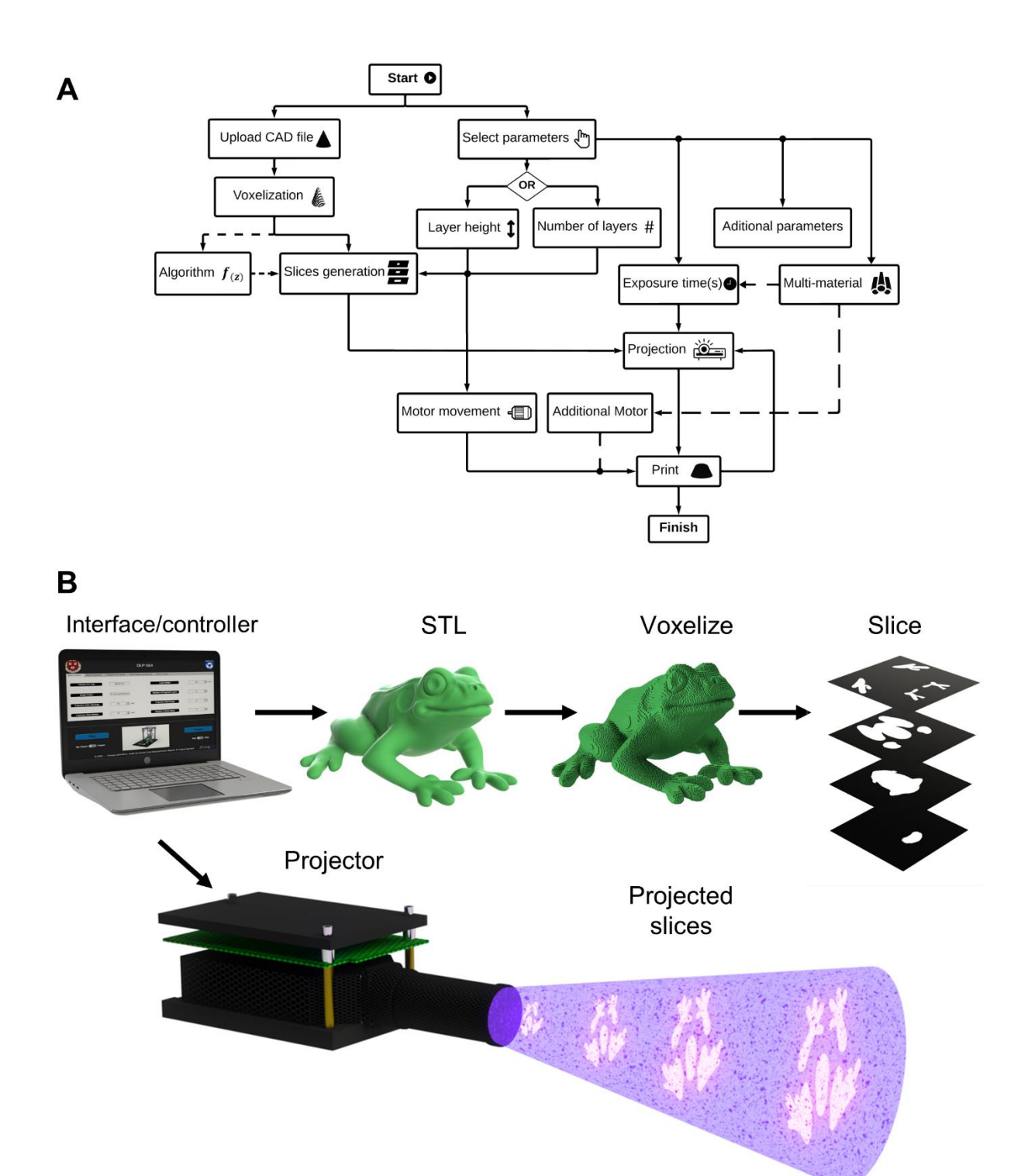


Fig. 7. Software architecture. A. Diagram flowchart of the functionality of a DLP bioprinter's software workflow. **B.** Graphical representation of the process of voxelizing, slicing, and projecting an STL file.

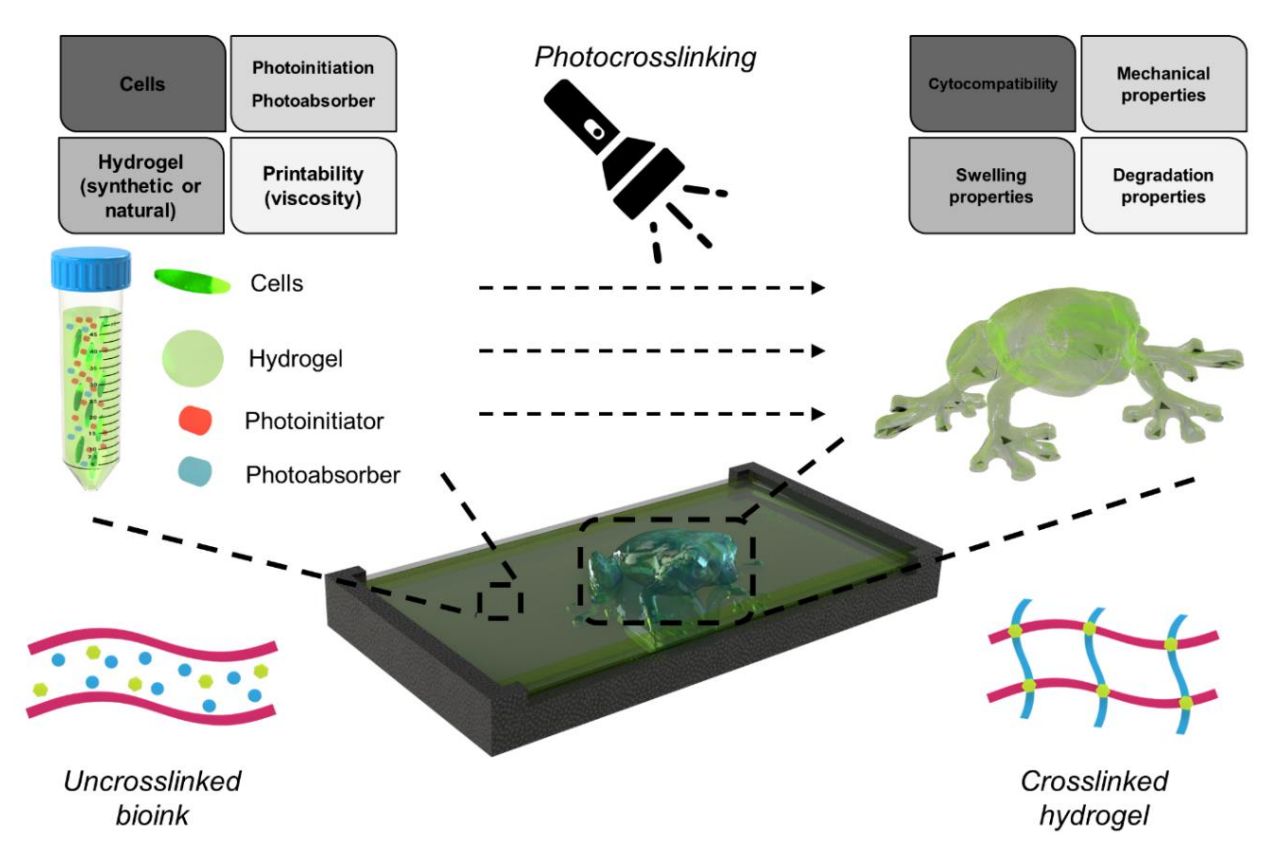


Fig. 8. Materials considerations. (Left) typical components that encompass uncrosslinked bioinks. (Right) main factors to control once the crosslinked hydrogel is obtained.